

1

2

3

Toward

4

multiscale modelling of

5

localised corrosion

6

7

8 **D.R. Gunasegaram, M.S. Venkatraman and I.S. Cole***

9

10 Commonwealth Scientific and Industrial Research Organisation (CSIRO)

11

12

13 *** Corresponding author**

14 Email: ivan.cole@csiro.au

15 Phone: +61 3 9545 2054

16 Fax: +61 3 9544 1128

17 Mail: Private Bag 33

18 CSIRO

19 Clayton South MDC VIC 3169

20 AUSTRALIA

21

22

23

Email addresses of the other authors

24 dayalan.gunasegaram@csiro.au

25 murali.venkatraman@csiro.au

26

Abstract

Localised corrosion is a cause of unanticipated and sometimes catastrophic failures of equipment, transport vessels and infrastructures. Therefore, the development of modern corrosion-resistant materials and inhibitors by design is both technically and economically attractive. In the coming decades, industrial components will be engineered from molecular structures. This prospect provides the designer with a truly enormous range of choices in design, which is a situation that demands predictive tools that can link molecular structures with the final component performance. In particular, the development of alloys and inhibitors can replace the use of toxic compounds in protecting metal surfaces. To execute a tailored design programme, it is necessary to understand how corrosion and the associated processes occur from the molecular level to the component level and how the overall system behaviour emerges because of the inherent links among different scales. Therefore, in the present work, the literature on theoretical modelling of localised corrosion and related experimentation are reviewed from a multiscale viewpoint. The review addresses (a) the challenges in the theoretical formulation of the important phenomena that influence localised corrosion and (b) the hurdles facing computational methods. It is shown that (i) the existing models lack the resolution to design effective corrosion-resistant systems, (ii) the numerical strategies for linking the scales are in a state of evolution and (iii) there are gaps in the experimental characterisation of the corrosion system, particularly at the lower end of the scales. Suggestions are provided towards the construction of a multiscale model for localised corrosion.

Keywords: localised corrosion, pitting corrosion, crevice corrosion, multiscale model, materials by design, density functional theory, inhibitors

List of abbreviations

1		
2		
3	ANN	Artificial Neural Networks
4	BEM	Boundary Element Method
5	BV	Balance Volume
6	CA	Cellular Automaton
7	GGA	Generalised Gradient Approximation
8	CCST	Critical Crevice Solution Theory
9	CSCT	Critical Solution Chemistry Theory
10	CVFEM	Control-Volume Finite Element Method
11	DFT	Density Functional Theory
12	DPD	Dissipative Particle Dynamics
13	DPDE	Dissipative Particle Dynamics with Energy Conservation
14	FDM	Finite Difference Method
15	FEM	Finite Element Method
16	FVM	Finite Volume Method
17	HFM	High Field Model
18	IRDT	IR Drop Theory
19	kMC	kinetic Monte Carlo
20	LCAO	Localised Combination of Atomic Orbitals
21	LDA	Local Density Approximation
22	LMPM	Lattice Material Point Method
23	MC	Monte Carlo
24	MD	Molecular Dynamics
25	MSM	Multiscale Model
26	OCP	Open Circuit Potential
27	PDF	Probability Density Function
28	QM	Quantum Mechanics
29	QSAR	Quantitative Structure-Activity Relationship
30	SIESTA	Spanish Initiative for Electronic Simulations with Thousands of Atoms
31	SPH	Smoothed Particle Hydrodynamics
32	VASP	Vienna Ab-initio Simulation Package
33	XPS	Photoelectron spectroscopy

1
2
3
4
5
6
7
8
9
10
11
12
13
14
15
16
17
18
19
20
21
22
23
24
25
26
27
28
29
30
31
32
33
34
35
36
37
38
39
40
41
42
43
44
45
46
47
48
49
50
51

1.0 Introduction

Localised corrosion is the accelerated attack of a passivated metal at discrete sites in a corrosive environment. In a metal, it may initiate because of (i) a breakdown of the otherwise protective passive film and/or (ii) the presence of metal surface heterogeneities, such as grain boundaries or inclusions. Localised corrosion poses challenges for detection, and once initiated, the damage propagates rapidly, which results in unanticipated and sometimes catastrophic failures of the materials [1]. Localised corrosion may induce significant repair, maintenance and replacement costs of equipment, transport vessels or buildings [2]. Therefore, a successful development of purpose-designed corrosion-resistant alloys and inhibitors may have significant commercial benefits.

It is conceivable that future materials will be engineered from individual atoms or molecules, and researchers will be able to design molecular configurations and processing routes to obtain the required performance [3]. Key elements of a material are being designed on the molecular level (e.g., inhibitors and their interactions with metal surfaces), and the complexity and dimensions of these deliberately designed molecular elements will presumably increase in the near future. However, molecular design will permit myriad combinations (and permutations) that require validation to determine the most effective combinations. Combinatorial and high-throughput methods [4] are accelerating the pace of material discovery and optimisation. However, although they are faster than the traditional methods, these techniques are not sufficiently rapid and typically generate data only in the laboratory with no clear method of linking to the in-service performance. Combining computational modelling with high-throughput methods can not only significantly increase the speed of material discovery but also provide a link to the in-service performance. Using computational design, designers will be able to access realistic predictions of the properties and the performance based on the actual microstructure and the operating environment. In this regard, computational modelling may be considered a vertex of a triangle, where the other two vertices are represented by experimentation and the formulation of theories [5]. This comprehensive approach is especially beneficial in studying localised corrosion, where the inherently low rates of material removal make experimentation a relatively lengthy process, even under accelerated conditions.

Localised corrosion is inherently multiscale (see Fig. 1) because the nucleation and the propagation of pits are affected by phenomena on vastly different length and time scales (e.g., the surface interactions at the atomic scale vs. the environmental conditions that are described in the continuum scale). Thus, the corresponding computational design must be based on a multiscale approach. Fig. 1 illustrates the length scales of local corrosion from environmental conditions in the continuum, i.e., the macroscopic length scale, (e.g., [6]) to the mesoscopic scale that defines the material microstructure and ultimately to the atomic scale in charge transport phenomena (e.g., [7]). Despite this complexity, as a design tool, an effective multiscale model (MSM) [5, 8-11] must seamlessly combine the continuum and the atomistic descriptions of matter [12]. Future design [13, 14] at the molecular level will require this type of MSM. From this perspective, in the current work, the literature on such topics as the theoretical modelling of localised corrosion, the numerical techniques, the experimental knowledge required for model inputs and validation, and the limitations in software are critically reviewed. Several thoughts that are relevant to the development of a suitable framework for an MSM are also provided, and the challenges in the development task are highlighted. To the best of the present authors' knowledge, there is currently no comprehensive MSM in the public domain that simulates localised corrosion in metals from the atomic scale to the continuum scale, although an example of a prospective type has recently been stated [13]. However, there are MSMs for glass [11] and carbon [8] corrosion.

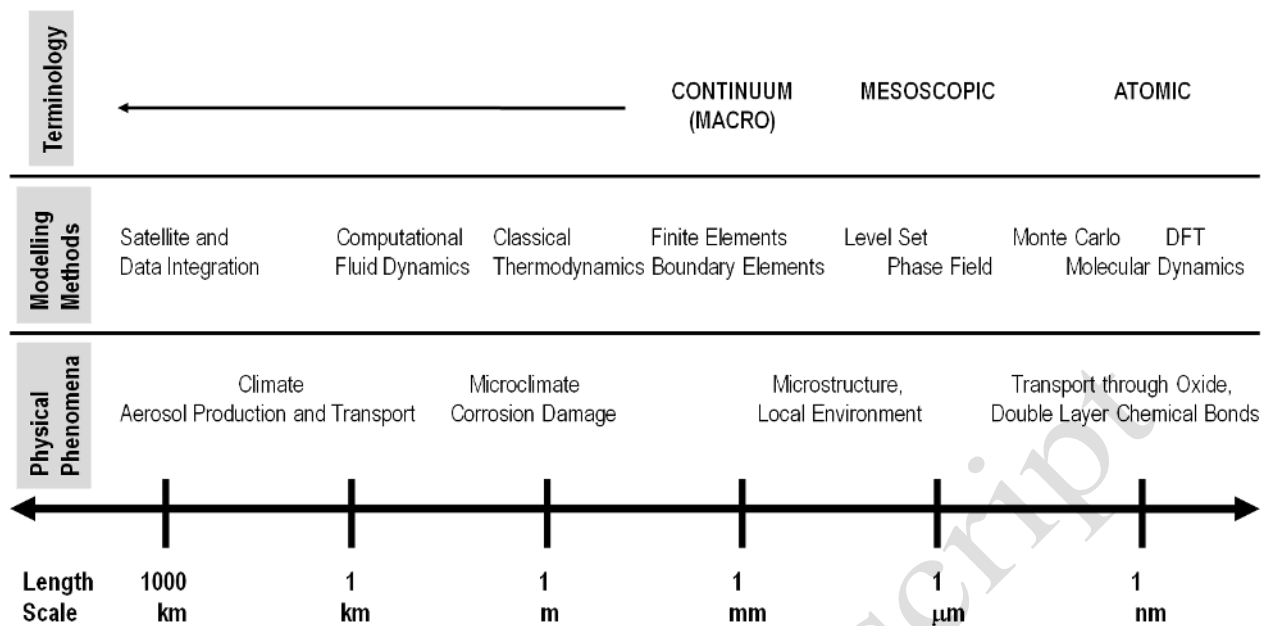


Figure 1: The spectrum of models to describe the electrochemical phenomena at various length scales (approximated)..

1
2
3
4
5

2.0 New paradigms for predictions

A prospective MSM on localised corrosion should provide more accurate and service-relevant predictions than the traditional approaches such as (i) the E-pH or Pourbaix diagrams (thermodynamics), (ii) the polarisation or Evans diagrams (kinetics) and (iii) the Nernst-Planck equation and the transport models that are based on the concentration solution theory. For example, the E-pH diagrams do not account for: (a) the transient behaviour (because they describe only the equilibrium states for given concentrations), (b) the localised variations in conditions such as concentration gradients, and (c) the highly influential features such as the alloy microstructure. Essentially, this thermodynamics-based empirical tool cannot be relied upon to predict the corrosion rates or the degree of passivity or for use in a non-equilibrium situation, although some useful extensions have been made [15] since its introduction. In addition, most Pourbaix diagrams only address pure metals and not alloys (an exception is Fe-Cr-Ni [16]). The polarisation diagrams do not consider mass transport limitations, which are important when there are concentration gradients in the electrolyte. In addition, different half-reactions (i.e., oxidation/ reduction) are activated at different potentials, and they depend on the microstructural features of the electrode and the microenvironment in the electrolyte; thus, several permutations and combinations of these polarisation curves are required to adequately describe an engineering system. Furthermore, the transport models heavily depend on the approximation of macro-homogeneity and local electroneutrality. Thus, the transport models neglect the atomistic details of the reactions and the inhibition mechanisms that occur on the metal or oxide surfaces. In addition, a common drawback of the above schemes is that they provide information at only one level. An ideal MSM should include strategies to overcome such limitations and the lack of resolution that accompanies the traditional techniques. For example, the alloy microstructure should be sufficiently described in terms of the metallurgical phases, their relative amounts, and their spatial distribution. However, to develop an MSM that provides a major advancement over traditional methods in the medium term, presently unavailable experimental data at the lower scales must be generated to describe the localised corrosion at an atomic level. Traditional electrochemical, surface analytical and spectroscopic studies only provide integral information on the electrochemical processes that occur at the solid/liquid interfaces, but they do not provide information on local atomistic events and the influence of surface imperfections on the interfacial processes [12]. In addition to such considerations, the MSM should seamlessly link the scales and be as computationally efficient as possible. In a recent review of MSMs in materials science, Elliot [5] noted that there are some promising strategies that are making progress at reducing the computational burden of models, in particular, at the lower scales. Thus, it is likely that a full-scale MSM can be solved within reasonable time frames in the not-so-distant future.

Types of existing models

3.1 Single scale models

Based on the assumptions about the behaviour of events (i.e., deterministic vs. stochastic) and the scales involved (atomic vs. continuum), currently, the available single-scale models may be divided into various categories (Table 1).

Table 1: Types of single-scale models that relate to localised corrosion.

	Main category	Sub category	Description	Example references
Categorised based on the assumptions relating to behaviour of events modelled	Deterministic	Atomic scale	Quantum Mechanics (QM) calculations are performed at the atomic level.	[17-21]
			Molecular Dynamics (MD) calculations are performed at the atomic scale	
		Continuum scale	Partial differential equations are solved using one of the following methods: analytical, Finite Element Method (FEM), Finite Difference Method (FDM), Boundary Element Method (BEM) or Finite Volume Method (FVM).	[22-30]
		Cellular Automaton (CA) models	In the CA models, the new state of a cell is a function of all states in the cell's neighbourhood at the previous moment in time. Most CA models follow deterministic rules to update the cell states (although the choice of the deterministic rule itself can be randomised)..	[31]
	Stochastic	Atomic scale	A Monte Carlo (MC) model that incorporates stochastic variability for the pit initiation and the pit widths.	[32]
		Continuum-Using Probability Density Functions (PDFs)	PDFs describe the likelihood that a pit would initiate at a given location at a given time under given conditions. PDFs are also applied in some cases for the pitting frequency, the pit incubation time and the pit generation rate.	[33-37] and review [38]
		Continuum - Using Artificial Neural Networks (ANNs)	The relationships between the causal parameters and the observed effects are developed without a deep knowledge of the physics. ANNs are criticised [39] for their "black box" nature, greater computational burden, etc.	[40-44] and review [45]
	Hybrid	Continuum scale	Combine elements of the deterministic models with those of the statistical models.	[46-48]

Currently, the deterministic models generally focus on the growth of a single, previously established pit (or crevice) or a collection of pits with predetermined anodic and cathodic sites. However, these models do not incorporate pit initiation events because the currently available experimental knowledge is insufficient to deterministically model the pit initiation, which is an atomic scale event

1 that is difficult to observe physically. Reigada et al. [32] note that this incomplete knowledge has led
2 modellers to consider pit initiation as a sporadic and stochastic event, whose random nature manifests
3 itself in both the distribution of induction time and the amount of current at a constant applied
4 potential. Furthermore, the computationally intensive molecular dynamics (MD) methods such as the
5 kinetic Monte Carlo (kMC) method are required to simulate atomistic events over distances that are
6 relevant to pitting. Therefore, the extents of the systems that may be covered in those simulations are
7 greatly limited, which reduces the practical value of such efforts, unless a multiscale approach was
8 employed. Regardless, given the expanding body of evidence that pertains to the preferential initiation
9 of pits at the microstructural features such as inclusions (e.g., [49]) and second-phase particles (e.g.,
10 [50]), it is increasingly likely that atomic scale deterministic models will be developed in the coming
11 years.

12
13 Although the stochastic models are elegant tools to model the mechanisms that are not fully
14 understood, ipso facto, they cannot be interrogated to gain a deeper understanding of the influences
15 that are exerted by causal factors. Thus, these models lack the resolution to define a process at the
16 level of detail that is necessary to design corrosion-resistant systems. In addition, the stochastic
17 models that the present authors found were developed in the macroscopic scale, except for the MC
18 model by Reigada et al. [32], which solved both the electrochemical responses and the morphological
19 features by assuming that the pit propagation is a tunnelling process.

20
21 The unified models (e.g., [46-48]) have sought to combine the elements of the deterministic models
22 and those of the statistical models to redress the limitations of the two approaches. For example,
23 Laycock et al. [47] developed an experimentally validated hybrid model, where a purely stochastic
24 model for pit initiation was combined with a deterministic model to propagate single pits in stainless
25 steel (SS). Such an approach is perhaps most suitable for the early versions of the proposed MSM.

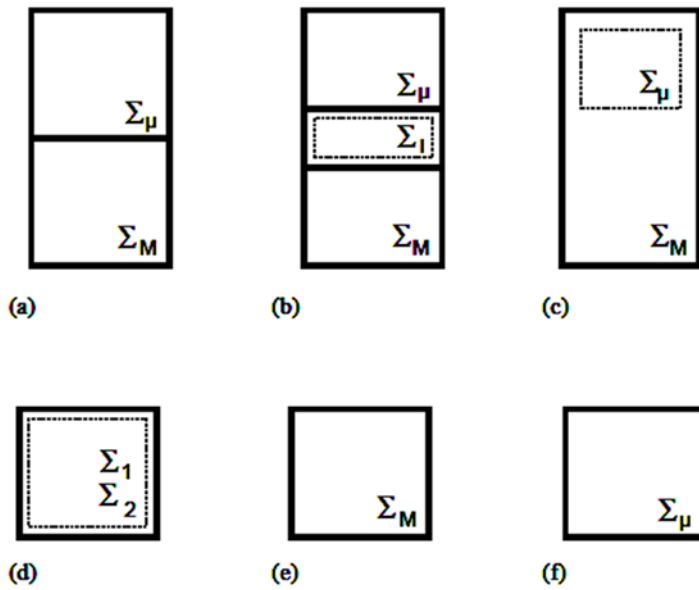
26 27 28 **3.2 Linking of the scales**

29
30 MSM may speed up computations by replacing the atomistic models with a less computationally
31 demanding continuum assumption at locations that are removed from the region of interest. In
32 addition, it extends material behaviour to the larger scales that represent the continuum realm. Thus,
33 an MSM makes predictions relevant to the engineers.

34
35 Ingram [9] has discussed different frameworks that may be adopted to link the scales (Fig. 2). This
36 figure shows how the two-scale domains may be linked in terms of the balance volumes (BVs) using
37 six different frameworks. The broken lines show the regions where such balance volumes overlap.
38 The BVs of the mesoscopic- and macroscopic- (continuum-) scale submodels are represented by \sum_{μ}
39 and \sum_M , respectively. In a multidomain model (Fig. 2(a)), the BVs occupy the adjacent, non-
40 overlapping parts of a system domain. In some cases, there is a small interface region between the
41 domains where both models apply (Fig. 2(b)). In an embedded framework (Fig. 2(c)), \sum_M spans the
42 system domain, whereas \sum_{μ} describes only a portion of that domain. In the parallel framework, both
43 models, which are labelled 1 and 2 in Fig. 2(d), span the system domain. In the serial framework (Fig.
44 2(e)), \sum_{μ} does not exist because the associated conservation equations are transformed into
45 constitutive relationships. Finally, in the simultaneous framework, the whole system domain is
46 described by \sum_{μ} . No balance volume is associated with \sum_M equations, since no conservation relations
47 are used at this scale. More details on these frameworks, including how information is transferred
48 between BVs, are provided by Ingram [9].

49
50 To circumvent the large computational load at the lower scales, the multiscale approach adopts coarse
51 graining towards the higher scales. For example, in an embedded MSM [9, 51], an atomistic model
52 may be embedded within a mesoscopic model, which can be embedded within a continuum scale
53 model. Then, the lower-scale model can update the higher-scale model at regular time intervals with
54 the corrosion damage information (e.g., [52] the simulating fracture). Moreover, one should also

1 consider the potential application of meshless methods [53-56] to pit propagation because these state-
 2 of-the-art techniques are being used increasingly successfully to simulate crack propagation (e.g., [53,
 3 54]) in the field of computational material science. These methods are better suited to tackle the
 4 moving discontinuities such as crack propagation along arbitrary and complex paths, whereas the
 5 traditional FEM methods would involve considerable meshing and re-meshing. There are significant
 6 inherent challenges in attempting to link the scales, and these challenges are well understood [5, 12].
 7 Elliot [5] and Tan [12] discussed several numerical methods that have been used for such linking at
 8 the boundaries of the two domains.. In Section 5.0, the present authors discuss the numerical
 9 difficulties that must be surmounted before a comprehensive MSM for localised corrosion may be
 10 successfully built.
 11



12
 13
 14
 15
 16

Figure 2: Framework class definitions [9] for the two-scale models: (a) multidomain, (b) multidomain (with interface zone), (c) embedded, (d) parallel, (e) serial, and (f) simultaneous.

4.0 Formulation of crucial phenomena

This section discusses the barriers and the data requirements for MSM, namely, the crucial parameters and events [57, 58] that influence the localised corrosion. This discussion on formulation ends with a pictorial summary (see Fig. 5 later) of the types of models that are currently used.

4.1 Microstructure of the metal substrate – its formation and influence

The microstructure of a metal or an alloy and its processing route control the sites of inclusions, the second-phase particles, the solute segregated grain boundaries, the flaws, the dislocations and the degree of surface roughness, all of which overwhelmingly influence the preferred locations for pit initiation. These quantities are discussed in detail elsewhere [15, 50, 59-61].

The present review suggests that the existing continuum models are too limiting in their treatment of the microstructure. However, there are early MSMs that may be used as starting points to build future MSMs which comprise microstructure evolution during solidification and link a microstructure to in-service performance.

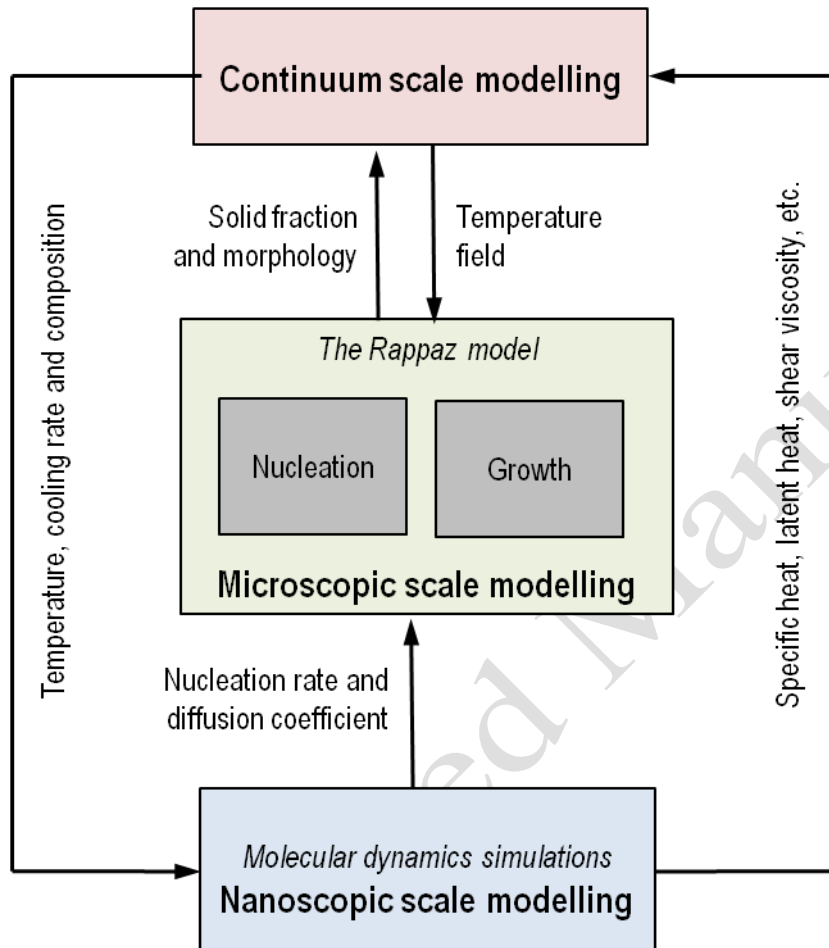
4.1.1 Continuum models – rudimentary description of microstructures

Several early single-scale (continuum) corrosion models (Sharland [62]) and many recent works (e.g., [29, 63, 64]) did not consider the microstructure. However, the modellers who did, assumed the microstructure as a given. The modellers who followed the deterministic path (e.g., [65-67]) have defined the microstructure either in their computational grids [65, 66] or treated them as a regular array and used analytical solution methods [67]. The modellers who work in the stochastic realm have used PDFs (e.g., [68]) to account for the probabilistic nature of the features. Brown and Barnard [65, 66] incorporated the microstructure that defines a certain electrochemical property (e.g., different Tafel dissolution kinetics for individual phases) for each Finite Difference Method (FDM) computational cell. Their latter model [65] could predict the distribution of cathodic regions. Jakab et al. [67] also developed a simplified deterministic model by treating a heterogeneous AA2024-T3 electrode as a regular array of Cu-rich favoured cathodic sites (partially covered with an inactive aluminium oxide layer) in a benign Al matrix.. Furthermore, Zhang et al. [68] developed a stochastic model for the same alloy AA2024-T3, which, according to the authors, provided a new approach to the prediction and the quantification of localised corrosion kinetics based on the alloy microstructure. Their PDFs for grain dimensions had parameters that were fitted based on the observed three-dimensional grain sizes, and a ‘brick wall model’ was used to model the grains (and the inter-granular regions) in 3D. There are also empirical models that correlate the corrosion consequences with the microstructural aspects. For example, Cavanaugh et al. [69] developed an empirical relationship between the accumulated corrosion damage in AA7075-T651 and the physical and electrochemical characteristics of the intermetallic particles, and this model predicted the pit radii (assuming hemispherical pitting) as a function of the immersion time in the 0.1 M NaCl. However, such models have limited applicability and cannot be relied upon for any experimental conditions other than those for which they were developed. In summary, the traditional continuum models that incorporate the microstructure have assumed it as a given quantity and have described it in relatively simplistic terms. No work appears to have considered details such as the recently observed [70] non-random clustering of buried intermetallic particles in AA2024.

4.1.2 MSMs for solidification and prediction of service life – early versions are promising

1 4.1.2.1 Microstructure evolution during solidification

2
3 The formation of microstructure originates at the atomic scale, where the initial nucleation and the
4 growth of critical nuclei occur [10]. This formation is followed by the growth of microstructure at the
5 intermediate mesoscopic scale. Rafii-Tabar and Chirazi [10] have reviewed several deterministic,
6 stochastic, hybrid models and some early multiscale models that predict the microstructure evolution;
7 they have also developed a well-documented, validated, generic MSM that spanned the nano-meso-
8 continuum scales for microstructure formation (Fig. 3).
9



10
11 **Figure 3: A multiscale model for solidification by Rafii-Tabar and Cherazi [10].**

12
13
14 Their MSM is representative of the limited number of available MSMs for microstructure prediction
15 that can be linked to an MSM for localised corrosion. In the Rafii-Tabar and Chirazi model (Fig. 3),
16 MD simulation techniques were used at the atomic scale and linked to a cellular-automaton (CA) -
17 based mesoscopic model for microstructures. The Rappaz model [71] that was used for the
18 microstructure combined a stochastic approach to the nucleation of grains (which was implemented
19 using CA) with a deterministic, diffusion-controlled approach to their growth. The parameters that
20 were used in the Rappaz model were calculated using MD simulations. Finally, the continuum scale
21 simulations were performed based on finite-element (FE) and finite-volume (FV) techniques. The
22 models at different scales were executed independently and coupled through databases using a serial
23 framework (Fig. 2(e)). The procedure was to associate an MD simulation box with a CA volume to
24 couple the nano-meso models, followed by associating a CA volume with a finite volume to couple
25 the meso-macro models. Because only one-way coupling is possible in a serial framework, and
26 because the three scale models were run separately using different codes, it was necessary to run the
27 meso and macro models more than once to achieve the two-way coupling between the scales through

1 iteration. For example, in its first run, the meso model generated the inputs for the macro model, and
2 in the second run, which was performed after the macro model had predicted the temperature
3 evolutions, it predicted the microstructure based on the temperature histories and the cooling rates.

4 4.1.2.2 Influence of microstructure on the in-service performance

5
6
7 The MSMs to link microstructure with the in-service performance at continuum scales for steel were
8 published by research teams that were led by Olson [72, 73]. From these MSMs, some concepts and
9 strategies could be borrowed to incorporate the influence of microstructure on the corrosion
10 performance at higher scales. The Olson models link the microstructure of steels with failure
11 scenarios such as ductile fracture by predicting the relevant properties. The microstructure was
12 decomposed into multiple scales using a nested domain framework (i.e., an extension of the
13 embedded framework, Fig. 2(c)). The continuum scale was linked to an embedded microscopic scale
14 (primary inclusion particles) and again to another embedded sub-microscopic scale (secondary
15 inclusion particles). Thus, their finite elements solutions could account for the influence of inclusions
16 during fracture in terms of the particle size and the carbide/ matrix debonding stress.

17 18 **4.1.3 Recent advances**

19
20 Amongst MSMs for solidification that span all scales, because the Rafii-Tabar and Chiraz model [10]
21 applies in its current form only to binary alloys, the important effect of the alloying elements on the
22 corrosion morphology [50] cannot yet be modelled. Therefore, the more recently developed and
23 validated MSM models [74-76] are more attractive for the corrosion modellers who work with
24 engineering alloys, although these models span only the meso to continuum length scales and the
25 associated temporal scales. These latter models are useful because they are capable of handling both
26 ternary [74, 76] and quaternary [75] alloys that are industrially more relevant. These 3D models can
27 also account for the influence and the interaction of multiple phases (solid/liquid/gas) during the
28 microstructure development. In addition, some of the latter models (e.g., Wang et al. [75]) have
29 further enhanced their realistic nature by accounting for the effects of the cooling rates and the alloy
30 content in their prediction of the microstructural features that included the shape, the size and the
31 distribution of the intermetallics and the defects such as porosity. The main output of these models is
32 typically a suggested deterministic microstructure. The information flow between the two levels in the
33 Wang et al. [75] model was facilitated through the coupling of temperature and pressure variables (see
34 Reference [76]). In addition, the lower-scale model was implemented as a subroutine of the macro
35 model, which was solved using FEM in an embedded multiscale framework (Fig. 2). The meso-scale
36 sub-region formed a total volume fraction of approximately 0.001% of the domain volume that was
37 covered by the continuum scale model, which allowed for the mesh sizes in the meso model to be on
38 the order of μm . In summary, the microstructure-evolution-related MSMs treated the nucleation
39 events stochastically (e.g., with a pre-set nuclei density and a nucleation potential with a Gaussian
40 distribution PDF [75]) and modelled the growth events deterministically using a hybrid strategy.
41 Thus, there is no purely deterministic microstructural model. Regarding MSMs for linking the
42 microstructure to the prediction of service life, validated works [72, 73] by Olson's teams appear to be
43 the most preeminent, and their strategies may be used as a basis to link the microstructure to the in-
44 service corrosion performance in MSMs.

45 46 **4.1.4 Proposed improvements**

47
48 Because the existing models on corrosion treat microstructure as a given quantity or have a simplistic
49 description of microstructure, the ability of an MSM (that incorporate such models) to tailor materials
50 is limited. An MSM on microstructure prediction should ideally be linked to an MSM on localised
51 corrosion, so that through a feedback loop, the alloy system may be optimised for corrosion
52 performance. Furthermore, none of the existing models account for the formation of the oxide layer
53 (Section 4.2 below), and they do not provide other corrosion-related information such as the
54 interfacial energies at the grain boundaries and the grain mismatch, which are indicators [77] of the
55 propensity of various sites to corrode in some cases. Therefore, in the long term, it is desirable to have

1 the microstructure model also predict the composition and the morphology of the oxide film.
2 Recently, promising efforts at atomistically simulating the precipitation kinetics in the solidification
3 of multicomponent interstitial/ substitutional alloys [78] have been published. It is also desirable to
4 predict the surface roughness characteristics. However, in the short term, the prescription of the entire
5 final microstructure as a given quantity remains a convenient starting point.
6

7 **4.2 Passivating oxide film, its thickness and its porous nature**

8
9 The phases that make up an oxide film that forms on the surface of a substrate are often traditionally
10 identified using Pourbaix diagrams [59], although these diagrams only describe the equilibrium phase
11 distributions. The passivating nature of the film is attributable to its limiting influence on charge
12 transport between the electrolyte and the substrate. The oxide film thickness varies between
13 nanometres (e.g., [79, 80]) and single-digit micrometres (e.g., [81]). Different oxides have different
14 degrees of stability depending on the environmental parameters [82] such as [81] the pH, the
15 corrosion product concentration and the ionic species. Almost all passive films have multilayer
16 structures, usually with the inner oxide and the outer hydroxide parts, the former is the barrier layer
17 against cation transfer, and the latter is an exchange layer with the electrolyte [83]. A review [7] on
18 passive films at the nanoscale has provided rare insights into the structure and the growth of oxide
19 films based on recently observed atomistic level details. In addition, the passivating films of Zn and
20 Fe are crystalline oxide grains with grain boundaries, whereas those of Al alloys and SSs are
21 amorphous in structure [84]. The electrochemical behaviour of the oxide film, its thickness and its
22 chemical composition depend on numerous parameters [79, 85-88]. Because this oxide film is
23 somewhat analogous to the artificial coatings [86, 89, 90] that are designed to decelerate corrosion,
24 some comments in this section are equally applicable to those coatings. The Pourbaix diagrams cannot
25 be accurately applied to passive films that are non-equilibrium structures, the existence of which
26 depends upon an appropriate relationship between the rate of formation and the rate of destruction
27 [91]. The recently introduced Kinetic Stability Diagrams (KSDs) [91, 92] may provide a means to
28 calculate the corrosion rates for alloys if they are further developed; however, their construction is
29 tedious because there are numerous possible combinations of electrode potentials, ionic
30 concentrations and pH.
31

32 The present review notes that the continuum models do not have sufficient resolution to describe the
33 atomistic mechanisms, and a lack of experimental data at lower scales makes it more difficult for
34 atomistic models to be developed in the short term to describe the behaviour of oxide films.
35

36 **4.2.1 Continuum models – lack resolution**

37 **4.2.1.1 Transport through the oxide film**

38
39 **Crystalline oxides:** Several continuum phenomenological growth kinetic models have been proposed
40 to model the growth of oxides and the rate-limiting cation-transport mechanism through the oxide
41 thickness. Many of these models have been reviewed by Hendy et al. [21]. All of these models
42 assume the homogeneity of the crystalline oxide to which they are applicable and have several free
43 parameters that must be fitted empirically. Hendy et al. [21] showed that by comparing their own ab
44 initio simulations with those of the phenomenological models, that the latter models were consistent
45 with the calculated barrier energies only if it was assumed that the grain boundary diffusion of cations
46 dominated. These results are consistent with the sentiments of Marcus et al. [28], who proposed that
47 the cations would preferentially migrate through the more electrically conducting inter-granular
48 regions. These findings highlight the importance of considering the grain boundary structure and their
49 inter-connectivity in the modelling efforts.
50

51
52 **Amorphous oxides:** For these oxides, models that relate to ionic conduction have been relatively
53 scarce. In a model that was proposed by Wang and Hebert [93], the current was carried by defect

1 clusters, which were created by the inward displacement of O^{2-} ions around an O vacancy in response
2 to the vacancy's electric field. The model hypothesised that the displacement created a gap between
3 the first layer and the second layer of O^{2-} ions that surrounded the vacancy, within which the metal
4 ions could easily migrate with little required activation energy. The analytically solved steady state
5 equations were satisfactorily validated using experimental results.

6 7 4.2.1.2 Interactions between the oxide film and the electrolyte 8

9 The interactions between the oxide and the electrolyte determine the rate of electron transfer
10 presumably by altering the electronic work function at the interface (e.g., Vago et. al [94]). However,
11 although phenomena such as O_2 reduction, oxide transformations and electron transfers to redox
12 species in a solution occur at an atomic scale, it would seem that atomic scale models are not yet
13 available in the public domain. Only continuum scale analytical models by Jakab et al. [67] and Chen
14 et al. [95] appear to address this phenomenon. In some cases such as the ZnO system, the ability of
15 oxides to act as reducing sites can significantly change the nature of the cathode and reduce the
16 diffusion limits [96]. For example, when $pH < 5$, the cathodic reactions in the Zn system are rate-
17 determining [61]. In such cases, the model must account for the scenario where the porous layer on
18 the metal surface either competes with or complements the oxygen reduction reaction (ORR) that
19 occurs on the metal surface. This scenario can be affected by many factors, and a recent continuum
20 scale porous-electrode model [97] has incorporated some of those influences. Nevertheless, an
21 atomistic-level deterministic treatment of the interactions is preferred because the mechanisms at play
22 operate at that level.

23
24 Although the metal surface can ideally be represented using a crystalline lattice, the oxide layer may or
25 may not be crystalline depending on the metal and the conditions under which the oxide is formed.
26 Most amorphous solids are initially hard, deform notably little, reach their plastic limit early and break
27 because they have a high strength and a low ductility ([98]). Multiscale modelling of amorphous solids
28 is far less advanced than in crystals because of the limited understanding of the behaviour of plasticity
29 in amorphous materials. The integrity of the oxide layer on an active metal is highly influenced by the
30 stresses that the metal beneath experiences. These stresses can locally rupture the oxide layer, which
31 leads to cracks (also known as holidays), through which the corrosive solution can percolate and reach
32 the surface of the metal. In addition, when the oxide layers host a cathodic oxygen reduction, the net
33 corrosion rate becomes vastly different from a situation where the oxide layers do not host such an
34 electrochemical reaction. FEM could ideally handle this situation in the continuum description. Note
35 that unless the oxide layer is electrochemically active, we may not be required to model the entire oxide
36 layer in a multiscale manner even if the oxide breaks down locally.

37 38 **4.2.2 Atomistic models and paucity of data at the atomic scale** 39

40 The continuum assumption of a uniform passivating layer for the complex heterogeneous structure of
41 the oxide film is quite inadequate. In addition, as noted by Williams et al. [99], although the
42 continuum models for migration and accumulation of point defects in the film are appropriate to
43 describe the behaviour of high-purity single-phase metals, they are inefficient for the engineering
44 alloys. Thus, atomic scale models are required. Maurice and Marcus [7] reviewed some of the
45 atomistic models and highlighted their usefulness in helping one understand the mechanisms that
46 occur at the lower scales. The ab initio model of Bouzoubaa et al. [18] predicted that the surface
47 undulations on the oxide film played a major role in its chloride thinning mechanism. Kim et al. [100]
48 used DFT to understand the origins of the natively n-type characteristics of ZnO by modelling the
49 interaction of a Zn interstitial with an oxygen vacancy. The 3D atomistic model of Diawara et al.
50 [101] successfully modelled the selective dissolution and the passivation of Fe-Cr alloys by
51 simulating the formation of oxide nuclei from chromium-rich clusters on the surface. This model
52 confirmed the experimental observation that Cr preferentially diffused towards the Cr clusters on the
53 surface, whereas iron atoms showed no such preferential diffusion. Their kinetic Monte Carlo (kMC)
54 model also showed that passivation occurred within a matter of seconds. The ab initio modelling work
55 by Costa et al. [20] on SSs studied the effect of water coverages in the Cr_2O_3 film on the surface, and

1 the energies of adsorption that it predicted were successfully validated with experimental data.
2 Similarly, Hendy et al. [21] calculated the energy barriers that were associated with the transport of
3 cations through the oxide film by combining ab initio simulations with experimental observations at
4 the atomic scale. These investigations reinforce the value in modelling the film at the atomic scale.
5 However, in this connection, Maurice and Marcus [7] noted that the development of such models will
6 be limited by the complexity involved in considering the three phases (alloy substrate/ oxide/
7 electrolyte), their interfaces, the electric field, the temperature, the orientation of the oxide film, its
8 nanostructural defects and the surface defects. The issue of heterogeneous passive films on
9 engineering alloys makes it critically important to select *what* is modelled. The examples above are
10 limited in terms of computational load when attempting to model engineering alloys even with a
11 reasonably low concentration (in relation to the number of atoms that can be considered in the ab
12 initio methods) of second-phase particles. This problem is even more challenging when pit initiation
13 is considered. Current ab initio models are rather weak at modelling the defects that exist at second-
14 phase particles in a matrix because the required number of atoms is too high.

15
16 The relative scarcity of models at the atomic scale is unsurprising given the computational burden
17 that we discussed above and because the experimentalists could not observe the oxide film in detail at
18 an atomistic level [28, 79] until recently. Nevertheless, there is an increasing amount of literature
19 (e.g., [79, 99, 102, 103]) that addresses such measurements, slowly filling the present gap in
20 knowledge at such length scales.

21 22 **4.2.3 Proposed improvements**

23
24 The oxide film is a classic example of the need for a multiscale approach to corrosion modelling
25 because its atomic scale thickness is coupled with its mesoscopic-scale microstructure, which is
26 punctuated with continuum scale defects. Thus, either a 3-scale approach or a less comprehensive 2-
27 scale platform (meso/ continuum scales) may be chosen to model the film. However, in the latter
28 approach, a generic phenomenological model that adequately describes in the meso or continuum
29 scales those mechanisms ([104, 105]) which actually occur in the nanoscale - through derived
30 transport and kinetic parameters - will be considered mandatory. The advanced version of a
31 prospective MSM should have the capacity to predict the oxide composition and structure (both
32 geometric and electronic), including its thickness and its porosity distribution, based on a given
33 microstructure of the substrate and the electrochemical environment. Of course, this hypothesis
34 assumes that sufficient experimental data become available for validation in the short to medium term.
35 For a deterministic model to have a strong predictive capability in relation to the electrochemical
36 behaviour of the oxide film, the following must be undertaken [106]: (a) the kinetic and the transport
37 parameters that are pertinent to different metallic constituents of the film must be determined either
38 based on the available values or using advanced experimental techniques, and (b) the energy
39 heterogeneity of the transport medium must be considered using the distribution functions for the
40 diffusion coefficients of individual species in the compact film and by quantifying the role of the
41 grain boundaries in the transfer of matter and charge through such a film. The model should also
42 account for the interaction between the film and the environment using kinetic data (and
43 thermodynamic data if the temperature influence is considered) on the adsorption, the surface
44 complex formation and the re-precipitation reactions of various cations at different pH levels and
45 locations of the oxide. It is also desirable that the atomistic modelling of nano-scale events such as the
46 oxide penetration/ thinning mechanism (e.g., [18, 28]), which leads to the prediction of nucleation
47 sites. In addition, some of the free parameters required for the phenomenological models may be
48 determined from first principles through such simulations where theories are available, rather than
49 being fitted empirically. However, given the enormous effort and time required to achieve all of the
50 above, the early versions of an MSM are likely to incorporate approximations for many of the
51 aforementioned aspects.
52

4.3 The influence of aggressive ions (pH and Cl⁻) and the role of inhibitors

The acidity or the alkalinity of the environment significantly affects the corrosion behaviour of metals, and there are several rules and exceptions that govern such behaviour [50, 57, 59, 61, 107]. Traditionally, the influence of pH on the corrosion tendency of metals in aqueous solutions of a given concentration has been described using the Pourbaix diagrams, the limitations of which have been mentioned in Section 2.0 (see also [92]). The inhibitor molecules in the electrolyte also significantly influence the corrosion rates, but unlike Cl⁻ ions, they slow down corrosion. Inhibitors are an attractive option when thick coatings are either unacceptable for isolating the metal from the electrolyte or when coatings may become damaged. In addition, inhibitors work by adsorbing onto the metal surface at its interface with the electrolyte [108] and creating nanometre-thick films instead of the usually millimetre-thick coating layers.

The current review found that the continuum scale models could not be used in a generic MSM because of their lack of generality, and the rapidly improving suites of atomistic modelling software packages are increasingly facilitating the modelling in this area at lower scales.

4.3.1 Continuum models – lack of universal applicability

Traditional models [25, 47, 62, 109-114] have either neglected the influence of pH or Cl⁻ or incorporated their influence in a rudimentary manner. Sharland [62] has reviewed some of these models. More recently, as noted by Frankel and Sridhar [115], a Point Defect Model (PDM) [116] incorporating empirically determined parameters correctly predicted the logarithmic dependency of pit initiation on Cl⁻ concentration, although it could not calculate the often observed bi-logarithmic dependence. The Cl⁻ influence was integrated in the PDM by hypothesising that its concentration altered the generation and the transport of cation vacancies. A simplified PDM for iron [117], which was based on the High Field Model (HFM) formulation, also predicted the correct qualitative trend for the dependence of the film thickness on the pH of the electrolyte. Nevertheless, neither PDM nor HFM can be universally applied (they are only valid for crystalline materials) and are limited by the assumptions (e.g., homogeneous oxide) and the need to fit the parameters empirically for each scenario. Lastly, the effect of the inhibitors has not been tackled by continuum models as much as the present authors are aware, which is understandable given the patent lack of resolution of such models in accounting for the surface/liquid interactions at the molecular level. In summary, traditional approaches such as the Pourbaix diagrams are inadequate, and the continuum models lack universal applicability and resolution in describing non-homogeneous microstructure. Thus, although some traditional models may have to be used in early versions of an MSM, a truly generic advanced MSM will require more detailed modelling at the lower scales.

4.3.2 Atomistic models – promising, but currently at early stages

The atomistic models of more recent origin have shown promise in this area by incorporating the influence of ions in the aqueous solution from a more fundamental point of view. Molecular or atomistic modelling brings to multiscale modelling a unique tool that can discriminate behaviour on the molecular scale [118, 119] and allow a molecular design. Consider the development of organic corrosion inhibitors. Their performance is strongly controlled by bonding (electron sharing) and the type of pendant functional groups that are attached to aromatic rings. However, the exact molecular structure has a critical impact on the inhibition performance; because conventionally, inhibition is measured by exposure of metal plates in inhibited solution or by electrochemical tests, a direct correlation to the inhibitor's efficiency does not exist because of the multiple scales that are involved. Hence, incorporating molecular modelling into a multiscale modelling framework offers the possibility of forming a continuous link from the molecular structure to the inhibition of anode and cathodic activity on the surface, which inhibits corrosion.

4.3.2.1 Density functional theory methods

A detailed account of the evolution of how the Schrodinger's equation is solved in DFT can be found in texts, e.g., [120]. In the modelling of surface/molecular interactions (such as inhibitors), the most commonly used basis sets are plane waves (see Table 2). The localised basis sets first approach (e.g., in SIESTA) the edge plane waves (e.g., in Quantum Espresso) because of the lower computational requirements that are associated with modelling the vacuum space.

Table 2: DFT software packages.

Package/Code	Available levels of exchange correlation approximation	Basis set formulation
VASP or Vienna Ab-initio Simulation Package	LSDA, GGA, Meta GGA, Hybrid	Plane wave
SIESTA or Spanish Initiative for Electronic Simulations with Thousands of Atoms	LSDA, GGA, Hybrid*	Linear Combination of Atomic Orbitals (LCAO)
Gaussian	LSDA, GGA, Hybrid	Gaussian Type Orbitals (GTO)
Quantum Espresso	LSDA, GGA, Hybrid	Plane wave

LDA - Local Density Approximation

GGA – Generalised Gradient Approximation

LCAO – Localised Combination of Atomic Orbitals

Taylor [121] has reviewed some works in this space. Bouzoubaa et al. [18] modelled the aggressive role of Cl⁻ in breaking down the passivity of the crystalline NiO using a periodic DFT. They intended to investigate the interaction of these ions with a stepped surface on the hydroxylated NiO film, which is characteristic of the barrier oxide layer on passivated nickel. The results suggested that adsorption of Cl by exchange with surface hydroxyls is energetically favourable but may not promote dissolution. Sub-surface insertion into the lattice was found to promote dissolution only if the Cl surface coverage was > 70%, which is unlikely because of the Cl-Cl repulsions. Thus, this work, which was performed on a defect-free surface, did not confirm the existing hypotheses of adsorption-induced surface thinning or Cl subsurface penetration. Bouzoubaa et al. later extended their work to include various halides [17]. Although a final word on the hypotheses cannot be provided until a more realistic surface with defects is simulated, the above works display the power of atomistic simulations besides putting conventional wisdom to the test.

4.3.2.2 Inhibitor/surface modelling

Inhibitors also have been modelled at the atomic scale by several workers (e.g., [122-129]), and the literature contains a wide range of approaches to model their interactions and electrochemical effects, some of which were reviewed by Gece [122]. In addition, although several software codes such as VASP, Gaussian and Quantum Espresso have been used, a relatively recent entrant known as SIESTA [128] appears promising in the area of inhibitors because its underlying method can describe well the interaction event. Much of the current work models the structures of inhibitors in vacuum [130, 131] and obtains the correlations [132, 133] with percent inhibition for a metal in an inhibited saline

1 solution. However, more recent studies [134] include solvation effects, examine an inhibitor's binding
2 to the surface, consider the charge double layer [135] and model the actual kinetics of the cathodic
3 reaction [124, 136]. The effect of solvation is considered by placing water molecules in vacuum.
4 However, two issues must be overcome [134]: a) the probable water structure must be estimated prior
5 to its placement (otherwise, the DFT code will spend all of its time to optimise the water structure),
6 and b) the long-range interactions such as hydrogen bonding and dispersion/Van der Waals forces
7 must be included. To include the dispersion forces, it is necessary to add an auxiliary force field to the
8 DFT calculation with a number of approaches that are developed to do so including: a) the non-local
9 functional (vdW-DF functional) of Langreth and Lundqvist [137], b) the modified pseudopotentials
10 (von Lilienfeld et al. [138], c) the highly empirical (hybrid) metaGGA functionals [139], and d) the
11 interatomic (pairwise or beyond) dispersion corrections such as that of Grimme [140]. The approaches
12 vary widely; for example, Langreth and Lundqvist explicitly incorporated the pairwise point-point
13 interaction while ignoring the non-additive many-body interactions, whereas Grimme's approach is a
14 highly empirical approach based on the parameterisation of the interaction energies.

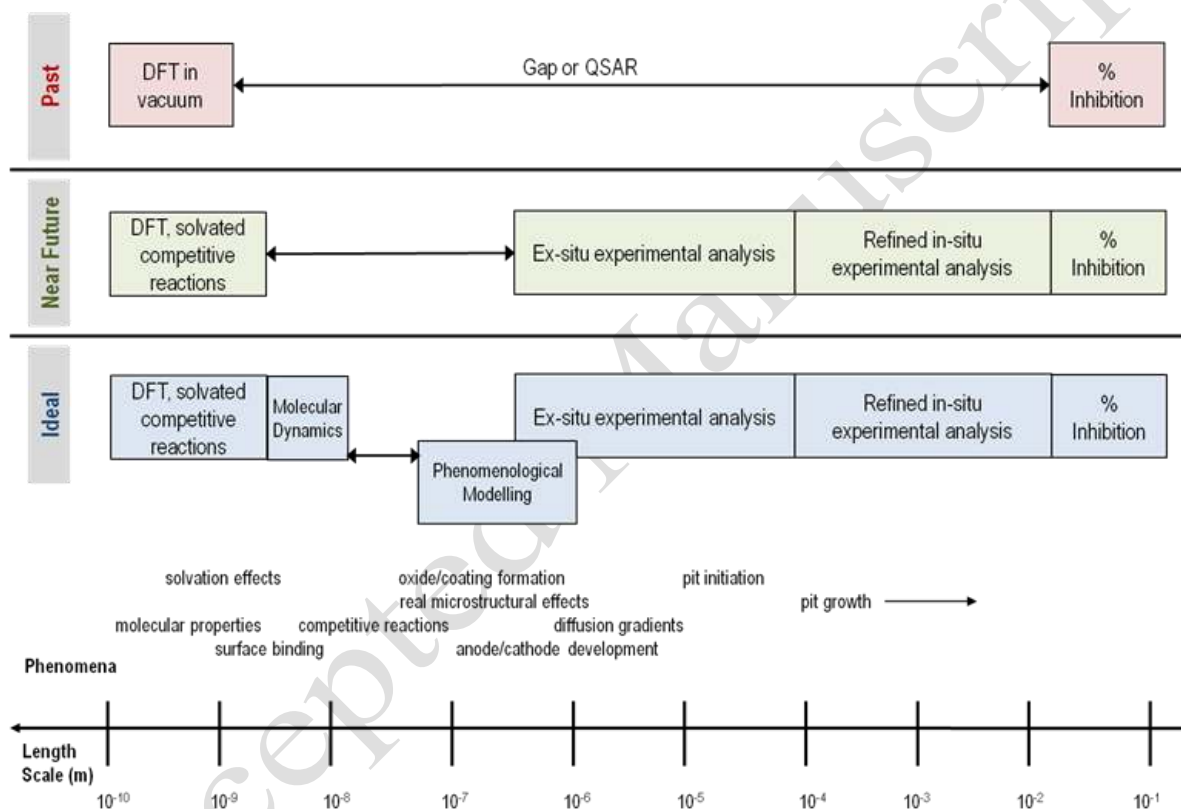
16 4.3.2.3 Modelling the electric double layer

17 Generally, the double layer effect on metal surfaces is modelled by adding or removing a charge from
18 the unit cell of the metal and balancing with a homogeneously applied counter [140]. This approach
19 can be problematic in plane-wave methods such as those used in VASP because the charge may not
20 be well localised. Spohr [141] has reported an increase in the use of ab initio models to simulate the
21 interfacial interactions between the electrolyte and the solid substrate by modelling the electric double
22 layer. One such work is by Taylor et al. [142], who examined the double layer regions for water over
23 a range of metals and compared the equilibrium potentials for the initial steps of water reduction and
24 oxidation at the surface with known experimental quantities. Spohr [141] and Yeh [143] found that
25 the inclusion of an explicit solvation provides more realistic reaction energetics in comparison to the
26 solutions in vacuum. Similarly, in a related work, Janik et al. [124] simulated the electronic double
27 layer by adding various numbers of electrons in a Pt unit cell and adding a compensating background
28 charge. However, Taylor et al. [144] noted that the effect of charge addition highly depends on the
29 orientation of water dipoles of the chosen solvation structure, and the fluctuations of the water
30 molecule orientation can induce instabilities in the charge localisation. This phenomenon allowed the
31 potential at the surface to be controlled by adding fractions of charge. They concluded that: (i) the
32 increasing use of molecular simulations allows the combination of statistical mechanical description
33 of the double layer with a description of elementary chemical processes on the electronic structure
34 level; (ii) the free-energy methods are applied to describe the chemical reactivity within and beyond
35 the framework of the continuum Marcus theory of electron transfer [145], and (iii) at sufficiently high
36 concentrations, direct simulations of the two-phase systems with an aqueous solution and a charged or
37 uncharged solid phase or surface can model the entire double layer region. Taylor [121] also
38 discussed the specific types of information that may be garnered from DFT simulations of various
39 metal-environment interactions and the associated challenges. To summarise, the atomistic models
40 that address different mechanisms at the electrolyte/electrode interface, including the influence of
41 ions, have begun to appear in the open domain and have provided useful insights into the interfacial
42 dynamics. In the large domain of inhibitors, although significant progress is being made, major
43 challenges must be resolved, including how to effectively model the solvation, the potential and the
44 chemical reactions at the double layer of the metal/solution interface.

46 4.3.2.4 Bridging the nano-gap

47
48 The design of inhibitors must span the scales from 10^{-10} m to 10^{-1} m (the scale of a test plate) and
49 cover a wide range of phenomena (see Fig. 4). The properties derived from DFT in vacuum studies
50 may not be relevant to the inhibitor surface binding and the link between the molecular properties and
51 the mesoscale phenomena such as anode/ cathode development, pit initiation, and pit growth is not
52 evident. Thus, a large gap currently exists between the DFT models and the measured inhibitor
53 efficiency in terms of both scale and phenomena. This gap is often [133] covered using a pattern
54 recognition or a neural network approach such as the Quantitative Structure Activity Relationships

1 (QSAR). In the near future, the DFT models will likely accurately include the solvation effects and
 2 model the competitive reactions (i.e., oxygen reduction vs. inhibitor absorption), and the local
 3 electrochemical techniques such as local EIS can be used to develop refined local parameters and their
 4 spatial variation (e.g., coating resistance or diffusional properties), whereas the post-test analytical
 5 procedures can examine the structure of the protective layers on the metal surface (i.e., using
 6 photoelectron spectroscopy (XPS), etc.) down to the sub-micron scale. Two additional developments
 7 can further close this gap. The DFT studies can be linked to MD studies, which will allow an order-
 8 of-magnitude expansion on the molecular scale [125]. Lastly, most electrochemical formulations are
 9 based on the Butler-Volmer equation, which provides an average free energy formulation of charge
 10 transfer but does not examine the individual processes that are involved in such transfer. Recent
 11 phenomenological models [146] break down the charge transfer in the solution into a number of
 12 components and allow each component to be addressed, which effectively refines the electrochemical
 13 scale.
 14
 15



16
 17
 18 **Figure 4: The “nano-gap” between the DFT models and the measured inhibitor efficiency.**

19
 20 At this point, a brief note about the use of ex-situ techniques such as XPS is appropriate. In such
 21 techniques, the specimens are removed from the experimental solution and placed in vacuum for
 22 examination. Such inspection under vacuum may significantly alter some aspect of the surface; for
 23 example, dehydration can occur, and the physio-sorption between the inhibitor and the surface will
 24 not be maintained, although chemical bonding and chemo sorption in particular will be. Thus, such
 25 techniques must be used with care, but they can provide valuable information.
 26
 27
 28
 29
 30

31 **4.3.3 Proposed improvements**

1
2 Based on atomic modelling, a more fundamental approach can be used for both crystalline oxides [21]
3 and the amorphous variety [147] and is well-suited to describe the solid/oxide bonding [148] and
4 oxide/electrolyte interactions [17, 18, 141]. This approach is likely the preferred option for a design-
5 optimisation MSM because of the fine resolution that it provides. There is currently no such
6 exhaustive and generic model, and until one becomes available, empirical correlations that are based
7 on mesoscopic and continuum scale models must be used to build an MSM. In the intervening period,
8 however, it may be possible to explore the use of KSDs to model the influence of pH and aggressive
9 ions at the higher mesoscopic and continuum scales. The current DFT work addresses the accuracy of
10 surface-binding studies and can also examine the competition between inhibitor binding and the
11 cathodic reactions. Hence, the objective of correlating DFT or MD [149] studies with a coarse
12 parameter such as the experimental inhibition efficiency may have to be modified in the light of data
13 from electrochemical and analytical techniques such as XPS, which probes the surface. Lastly, most
14 electrochemical kinetic models are based on the Butler–Volmer equation, which provides an average
15 free energy formulation of charge transfer but does not examine the individual processes that are
16 involved in such transfer. The proposed MSM should also address the commonly used but inaccurate
17 assumption that uniform conditions exist in the bulk solution; for example, this assumption often
18 neglects the concentration gradients that extend into the bulk solution from a pit or a crevice.
19
20

21 **4.4 Establishment of anodic and cathodic sites**

22
23 Anodic and cathodic sites are characterised by different potentials because of the variations in
24 chemical composition encountered in the alloy and/or the electrolyte. These two quantities (i.e.,
25 potential and composition) are coupled in the electrolyte through the Nernst equation under
26 equilibrium conditions. For a large cathode area with a small anode area [150], the distance between
27 these sites [151] and the protective films that formed on their surfaces affect the corrosion rate. A
28 small anode area results in the rapid penetration of the pit or the crevice because the current density at
29 the small anode is notably high, and the anodic polarisation in chloride solutions is extremely limited.
30 When the cathode size is limited [22], the limiting corrosion current is determined by the size of the
31 cathode (e.g., [152]). The establishment of the anodic and cathodic sites is dictated by several factors,
32 which are mentioned elsewhere [59, 61, 69, 150, 153-158].
33

34 The present review suggested that the continuum scale models lack the necessary resolution to
35 describe anodic and cathodic sites and that the development of more suitable atomistic models will
36 need to be supported by the generation of experimental data at the lower scales.
37

38 **4.4.1 Continuum models - contain limiting assumptions**

39
40 The continuum philosophy considers that whilst the potential difference on the corroding surface is
41 zero, there are anodic partial currents across the metal-electrolyte interface at microscopic surface
42 sites, the total of which is balanced by an equal value of the total cathodic current that is similarly
43 distributed under free corrosion conditions. This balance is achieved at the open circuit potential
44 (OCP) of the “homogeneous” metal substrate, and is determined by the rates of the partial
45 electrochemical reactions [159] (which are described by either the Tafel or the Butler-Volmer
46 equations). This information is sufficient for modelling the O₂ reduction-driven cathodic tendency
47 only when the influence of the microscopic inclusions and the alloying elements are ignored. There is
48 a limited number of continuum works (e.g., [160]) that address the anode-cathode separation, and they
49 are rudimentary. A model that automatically predicts the anode-cathode separation by solving the
50 mixed potential problem was developed by Venkatraman et al. [64] for corrosion under a
51 differentially aerated NaCl droplet, which was deposited on a Zn substrate. The surface was assumed
52 to be homogeneous; thus, no microstructural details were considered. The previously visited model of
53 Brown and Barnard [65] could predict the cathodic regions. More recently, researchers have started to
54 address the microstructural inhomogeneity-driven phenomena that are relevant to the anode-cathode

1 separation in alloys, e.g., the previously discussed model of Jakab et al. [67] (Section 4.1). In addition,
2 Alodan [161] simulated O₂ reduction using an approximated alloy-like microstructure and employed
3 circular discs for the cathodes (inclusions), which were surrounded by an annulus-like region for the
4 anode (aluminium). Although these latter models represent a step forward in the simulation of
5 engineering alloys, they still suffer from the over-simplification of the microstructure. Valutrin-UI et
6 al. [31, 162] developed a cellular automata (CA) -based mesoscopic model with a random walk of H⁺
7 and OH⁻ ions, where the spatial separation between the anodic and the cathodic sites could be made
8 smaller than that in the continuum scale; thus, the model could more realistically locate discrete
9 cathodic and anodic sites as interwoven within a propagating pit (i.e., not only on the side walls)
10 based on the solution pH at the mesoscopic vicinity. This model was unlike most continuum models,
11 where the cathodic sites are usually located outside the anodic pit or crevice or simply assumed to be
12 along the side walls of a pit. Although it constituted a step up from the continuum scale models in
13 terms of details, the model still lacked the resolution to handle the microstructural details of
14 engineering alloys and was limited by the approximations that described atomistic phenomena at the
15 mesoscopic scale. Therefore, lower-scale models must be developed for the anode-cathode
16 separation; any continuum treatment that assumes homogeneity in the microstructure is inadequate for
17 design purposes.

18 19 **4.4.2 Paucity in atomistic models and experimental data**

20
21 Atomistic models were difficult to find for this topic. However, because characterisation studies (e.g.,
22 [50]) have started to generate relevant kinetic data in the form of polarisation diagrams for different
23 alloy phases at the mesoscopic level, such models may soon be developed. An alternative that does
24 not depend on experimental data is an atomistic model that is constructed bottom-up from first
25 principles. No such model appears to exist in the current open domain for metallic corrosion, except a
26 model that is a part of a recent MSM by Yu [11] for glass corrosion. This situation is likely to change
27 with the generation of physico-chemical data at the atomistic level (e.g., energies for surface
28 formation, chemisorption, and adsorption) and the increasing application of high-resolution
29 characterisation techniques for corrosion-related studies (e.g., [79, 102]). Advancing observation
30 techniques such as the in-situ atomic scale studies that were reported by Magnussen et al. [163],
31 where the local removal/addition of atoms at atomic kinks at the steps of Cu crystal surfaces during
32 dissolution in 0.01 M HCl were observed and quantified, also serve to help accumulate knowledge at
33 lower length scales. However, until a sufficient amount of such data exists, the microstructure-based
34 empirical rules (e.g., for dissolution rates, such as the combination of a chemical rate law (first-order
35 law based on [H⁺]) and an electrochemical law (Butler-Volmer equation) as used by Suter et al [49] for
36 MnS dissolution in NaCl) may be necessary. These rules should also quantify the effects such as the
37 probable catalysis by [Cl⁻] of the MnS dissolution, which was proposed by Williams et al. [164], and
38 any possible influences of the oxide films.

39 40 **4.4.3 Proposed improvements**

41
42 One of the reasons for the lack of atomistic models might be the difficulty inherent in coupling the
43 electron transfer (current flow) between atomistic models of anode and cathode. The problem arises
44 because, at the atomistic level, calculations are typically performed for equilibrium configurations
45 whereas the formation of anode and cathodes are highly dynamic events. It is suggested therefore that
46 the potential use of fluctuation theorems [165] be considered for simulating the non-equilibrium
47 mechanisms. The central premise of these theorems revolves around comparing the probability of
48 phase-space trajectories of the system with that of the anti-trajectories (one that the system would
49 traverse if it were moving in the negative time direction), thus introducing the concept of time-
50 irreversibility into the continuum processes. Thus a non-reversible, non-equilibrium process such as
51 corrosion may potentially be modelled using fluctuation theorems at the mesoscopic level, facilitating
52 the prediction of the evolution of favourable phase-space trajectories. Fluctuation theorems are
53 discussed in more detail later, in section 5.3. Early versions of an MSM are likely to have varying
54 degrees of approximations to simulate the anode-cathode separation. One of the available avenues for
55 the development of such models is perhaps the extension of models like that of Diawara et al. [101],

1 discussed earlier in Section 4.3, and that of Legrand et al. [166]. These models simulate the selective
2 dissolution of Fe and the passivation of a cluster of Cr atoms (which simulates the Cr₂O₃ layer) in Fe-
3 Cr alloys. Another pathway is available from the previously noted work of Yu [11], who simulated
4 the corrosion of glass. This MSM had an atomistic model that was coupled to an MC simulation of
5 surface phenomena such as hydroxylation with cations, chemisorptions, adsorption and dissolution.
6 Then, the continuum scale phase field simulations were performed using material properties that were
7 fed from separate MD simulations. Although the MSM contained approximations and educated
8 guesses and at times relied upon empirically obtained parameters, its framework provides a potential
9 platform for the development of an MSM for localised corrosion.
10
11

12 **4.5 Metastable pitting**

13
14 Metastable pitting is generally accepted as the necessary precursor to a stable pit initiation in metallic
15 systems that include SS [167], aluminium [88] and cast iron [168]. This stage is characterised by the
16 consecutive formation and repassivation of sub micrometre-size pits below the OCP of an alloy,
17 which leads to oscillations in the potential transients in the active direction in an open circuit during
18 the incubation period for stable pitting [57, 88]. Some of the metastable pits survive beyond their
19 usual lifetime of the order of seconds [57] and grow to transition into stable pits under favourable
20 circumstances, which are mentioned elsewhere [25, 50, 88, 167]. Recently, additional causes such as
21 clustering have been suggested to encourage the transition [169-171]. The phenomenon has attracted
22 several theories, including those reviewed by Frankel [172]. In short, from the works of Burstein et al.
23 [173] and those of others (e.g., see Frankel's comments on Sand's equation), it would appear that the
24 metastable pits thrive as long as a critical solution chemistry is maintained using various means([173],
25 [174]). However, they would die through repassivation following a change to this chemistry, which is
26 precipitated by a catastrophic event such as the loss of the cover at the pit mouth or a violent rupture
27 of the passive film covers, leading to a mixing with the bulk solution. Experimental scientists who
28 work with alloys have reported other conditions that can lead to metastable pits (see [50], [175-179]).
29

30 The present review did not find any atomistic models, although pit nucleation is essentially a
31 nanoscopic event. It was observed that because of an inability to adequately account for the
32 microstructure at the required scale, the continuum models largely depended on a stochastic treatment
33 of the subject.
34

35 **4.5.1 Continuum models - mainly stochastic**

36
37 Because the triggers for the initiation of metastable pits and their repassivation or transition to the
38 stable pits were poorly understood deterministically, a stochastic model that was proposed by
39 Williams et al. [36] based on a treatment by Shibata [180] has been frequently used. Experimental
40 data analysis is required to fit this model to a particular system [36]. However, this model
41 simplistically assumed that each micro pit had an equal chance of propagating into a macro pit, which
42 disregarded the role played by the microstructure, the local microenvironment and any aspect of the
43 pit itself, e.g., the narrowness of the mouth or the existence of a pit cover. Nevertheless, it is
44 interesting that the likelihood of interactions between the metastable pits, which were recently
45 observed using *in situ* techniques at the micrometre scale [170, 181], were actually predicted by a
46 stochastic model by Wu et al. [37], which pre-dated the observations. By assuming through a
47 "memory effect function" that each pitting event will influence subsequent events and the influence
48 would exponentially decay with time, that model could successfully reproduce the current transients
49 that were recorded during the metastable pitting of an SS alloy and an aluminium alloy. (However, it
50 must be noted that the current transients may also be caused by events such as trenching or de-
51 alloying). This temporal model was subsequently extended to a spatiotemporal version by Organ et al.
52 [182]. However, the model remained limited by the assumption that the surface was homogeneous
53 without any preferred sites for nucleation because the microstructural effects were not modelled. A

1 model developed by Walton et al. [183] (which is discussed later in Section 4.6) appears to be one of
2 the first model that accounted for the active/passive transition based on the potentials. The Cellular
3 Automaton (CA) models [184, 185] that addressed metastable pits concluded that their growth is
4 controlled by the anodic dissolution probability. Other models of note are by Malki and Baroux [186,
5 187] and Hoerle [188]. In summary, the continuum models that accounted for metastable pitting were
6 stochastic in nature and did not consider the influences of microstructure or other factors such as ions
7 (the Cl^- ions were neglected). They also did not account for the non-random nature of some features
8 such as the intermetallic particles in some aluminium alloys, which were found in clusters instead of
9 being arbitrarily distributed [70].

13 4.5.2 Proposed improvements

15 The present authors did not find any atomistic model that addressed metastable pitting. The common
16 drawback among the existing continuum models is that none of these consider the microstructural
17 effects despite their significant influence [189]. Therefore, an MSM should comprise a meso-scale
18 model that adequately describes the microstructural features, which affect the metastable pitting,
19 including the mechanism of active/ passive transition if possible. An MSM should also be able to
20 handle the differences in the behaviour of the current transients between systems, such as SS and
21 aluminium (see [190]), and such events as co-operative spreading [169, 170]. In addition, because the
22 pit nucleation events occur at the nanoscopic scale [10], an MSM that incorporates metastable pitting
23 should preferably include a model at this length scale, but a stochastic approach may be used for the
24 initiation phenomena until such model is available.

27 4.6 Stable pit initiation

29 Pitting is caused by the localised failure of a passive oxide film [191] or the selective dissolution of a
30 grain boundary or an inclusion [50] on a metal surface exposed to an electrolyte, and it is
31 characterised by accelerated corrosion in the local region. For instance, it is generally agreed that
32 anodic dissolution of MnS inclusions results in a change of the local solution composition near the
33 inclusions, resulting in a condition where the passive film on the SS surface can no longer be
34 sustained [192]. In general, most pits nucleate if the potential of the alloy surface is above the
35 nucleation potential (or film breakdown potential or pitting potential) for the local electrochemical
36 environment. After an incubation period, a pit propagates if the surface potential remains above the
37 pitting potential. Especially in alloy systems involving SSs [99, 167] and aluminium [88], some
38 metastable pits nucleate at potentials that are hundreds of mV below the OCP and eventually
39 transition into stable pits (Section 4.5). Therefore, the proposed MSM should allow either path for pit
40 initiation. However, there are unanswered questions about the exact nature of the events that trigger
41 pit initiation [79, 99] and the mechanisms associated with film breakdown [172]. According to Kempf
42 et al. [79], highly sophisticated techniques are required to study pit initiation events on sub-
43 micrometre scales. High-resolution observations are, however, increasingly becoming commonplace,
44 allowing informed theories to be developed. For instance, Marcus et al. [28] observed experimental
45 data on the nanometre scale and proposed mechanisms for pit initiation at inter-granular regions.
46 Other similar observations were reported recently by Magnussen et al. [163] and Williams et al. [99].
47 Reviews of the critical factors affecting the pitting corrosion of pure metals and alloys are readily
48 available, e.g., [115, 172, 193].

50 The current review determined that in the absence of a consensus on how pits nucleate, various
51 continuum models have taken different approaches. While the results of atomistic models are
52 encouraging, additional experimentation on smaller scales is required to facilitate a convergence of
53 views on this controversial topic.

4.6.1 Conventional theories – insufficient mechanistic detail

Two conventional theories encapsulate the traditional deterministic criteria: (a) critical solution chemistry theory (CSCT) or critical crevice solution theory (CCST) [194-196] and (b) ohmic resistance-based IR drop theory (IRDT) [63, 197]. According to CSCT/CCST, passive film breakdown occurs when the pH and the Cl⁻ concentration reach a critical state. However, according to IRDT, localised corrosion starts abruptly when the electric potential drop (IR) between the mouth and the interior of a pit or crevice is large enough to activate anodic potentials. Shortcomings of IRDT have been discussed by Frankel and Sridhar [115] and others (e.g., [198, 199]). Although CSCT/CCST has been supported overwhelmingly in the past, a recent attempt [63] has been made to develop and validate a model that unifies CSCT/CCST and IRDT. However, all of these theories are for pure metals and ignore the seminal role played by microstructural inhomogeneities (including surface roughness) on pitting initiation on engineering alloys. For example, neither of these theories includes the preferential dissolution of select alloy phases as a cause of pit initiation.

4.6.2 Continuum models – multiple approaches

As mechanisms relevant to pit initiation take place on the atomic scale, the continuum treatment involves significant approximations and assumptions. In addition, the absence of a consensus view on pit initiation is reflected in the variety of approaches that have been used to model pit nucleation. Many of these studies have been reviewed by Sharland [62], Frankel [115, 172], Kennell et al. [63], Papavinasam [200] and Anderko [15], but a small sample of this research is discussed here. Anderko [15] reviewed several theories for passivity breakdown and concluded that all of them share a common theoretical result: the passivity breakdown potential varies with the logarithm of the concentration of aggressive ions, which is confirmed by experimental data. He also notes that, while this observation is accepted widely, its generalisation to systems with multiple types of aggressive and inhibitive ions is not obvious. Given the poorly understood nature of pit initiation mechanisms, it was convenient to use a stochastic approach to model pit nucleation (e.g., references in [38], [34-37]). Hybrid models (discussed in Section 3.1) typically take a stochastic approach to model pit initiation (e.g., [46-48]). These formulations calculate quantities such as pit birth rates based on probabilities or assumed statistical distributions rather than physically viable mechanisms. A common feature of stochastic models is that physical mechanisms (e.g., for passive film breakdown and pit initiation and growth) and microstructure are not included explicitly. These considerations limit the applicability of stochastic pit initiation models for alloy design. The pre-eminent deterministic models are the 1D steady-state models by Galvele [194-196] – the proponent of CSCT/CCST – that influenced deterministic thinking for decades by providing a step change in the ability to rationalise experimental results in various systems. However, as Newman [201] notes, the Galvele approach needs minor revisions to include highly concentrated metal salt solutions in pit nuclei. Other significant deterministic models are those of Alkire and Siitari [202], Sharland [203], Laycock and Newman [204], Cong et al. [205] and Walton et al. [183]. The transient 1D model by Walton et al. was one of the first that considered the electrode kinetics of both cathodic and anodic reactions with active/passive transitions. An electrode kinetic model developed and validated by Mccafferty [113] took into account the adsorption of chloride ions on aluminium oxide surfaces, the penetration of chloride ions through oxide films, and the localised dissolution of aluminium at the metal/oxide interface in consecutive one-electron transfer reactions. The 1D pseudo-steady state model of Webb et al. [192] modelled the influence of MnS inclusions on SS surfaces. However, all these continuum models suffer from the shortcomings discussed in Section 4.6.1.

4.6.3 Atomistic models – showing promise

Decades ago, Williams et al [206] attempted to develop an atomistic model of pit initiation on random binary Fe-Cr alloys. They added a scheme for passivity breakdown based on CCST to existing atomistic models [207, 208] by postulating that passivity breakdown corresponds to the critical chemistry necessary for the activation of the alloy. Their model identified the most important factors for pit initiation on SS: (a) the dissolution probability of Cr atoms; (b) the alloy composition, which

1 determines the cluster size distribution; and (c) diffusion and migration within the cluster volume. A
2 more recent atomistic work by Bouzoubaa et al. [18] has proposed tenable mechanisms of passivity
3 breakdown. Currently, experimental observations are being made on the atomistic scale – e.g., the
4 recent observations of aluminium oxide by Zavadil et al. [105]. Rashkeev et al. [209] have performed
5 first-principles quantum-mechanical calculations to provide an atomistic understanding of corrosion
6 initiation on Al under atmospheric conditions. Their results suggest that atomic hydrogen penetrates
7 oxide films and causes structural damage in oxides and at Al/Al₂O₃ interfaces. To summarise,
8 atomistic modelling increases the understanding of pit nucleation by modelling mechanisms on their
9 characteristic scales. Therefore, atomistic models are most suitable for modelling pit initiation.

11 4.6.4 Proposed improvements

12 Nucleation events are best modelled on atomic scales, and appropriate models have started to become
13 available. These models, however, are still in their infancy and only explore probable mechanisms for
14 pit nucleation, which remains a controversial topic. More investigations, like the X-ray photoelectron
15 spectroscopy studies and MD simulations of amorphous Al₂O₃ by Chang et al.[210], may illuminate
16 the relationship between oxide structures and passivity breakdown. First principle quantum
17 mechanical calculations such as those carried out by Rashkeev et al. [209] and Scully et al. [171] may
18 provide an alternative to experimentation until better techniques become available for observing pit
19 initiation events. However, until a deterministic model is developed for pit initiation, MSMs on
20 localised corrosion may use stochastic models. It is necessary to prescribe the microstructure to apply
21 the early deterministic models to the selective dissolution of inclusions/second phase particles at rates
22 based either on empirical polarisation curves (e.g., [50]) or dissolution models (e.g.,[25, 49, 211]).
23 The effect of microstructural roughness can be incorporated by drawing from, for instance, the
24 empirical relationship between surface roughness and pitting potential (e.g., [212]). If continuum
25 deterministic approaches are adopted until models on mesoscopic scales are available, other
26 approximations may be required, for example, Olson et al. [213]. They considered that surface energy
27 must affect pit formation and treat pitting corrosion as a nucleation and growth process where surface
28 energy promotes an activation barrier.

32 4.7 Pit or crevice propagation and rate

33 Pit growth is autocatalytic in nature in that alterations in local conditions [57] promote the further
34 growth of a pit in its propagation stage. (These environmental changes are considered in Section 4.8.)
35 The spatial separation between the anodic and the cathodic reactions results in a negative pH gradient
36 between the pit and the film that sustains the electrochemical reactions. Factors that control pit growth
37 rate are discussed by Frankel [172]. Whilst the initiation and early metastable growth of a pit are
38 activation controlled (Butler-Volmer or Tafel kinetics equations), pit or crevice propagation above the
39 pitting potential is mass transfer controlled [199] (Nernst-Planck equation). For an activation-
40 controlled reaction, the current density is plotted on a polarisation plot (potential E vs. \log (current I))
41 or Evans diagram. Current density in a pit is a measure of the corrosion rate in the pit and, thus, a
42 measure of the pit penetration rate [57]. Pioneering modelling work based on CSCT/CCST by Galvele
43 [194, 195] showed that a critical value for the product of the current density i_{corr} with the pit depth x ,
44 the pit stability product $= x \cdot i_{corr}$, may be found in terms of the concentration of the ionic species at the
45 bottom of a one dimensional pit. This critical $x \cdot i_{corr}$ value corresponds to a critical pit acidification
46 condition for sustained pit growth, and it can be used to determine the i_{corr} value necessary to initiate
47 or sustain pitting at a defect of a given size [57]. However, because Galvele's treatment explicitly
48 ignores the effects of cathodic reactions inside the pit, it is only relevant at potentials well above the
49 OCP of the metal in its critical localised solution. A topic that remains controversial is the degree of
50 influence exerted on pit propagation by salt films that form on electrodes when the dissolving cations
51 and, say, Cl⁻ ions combine at saturation concentrations of the salt in solution [204]. Another
52 unresolved subject is the formation of lacy covers on pits on SS that limit diffusion at pit mouths and
53

1 thus help to maintain the critical chemistry in the pits. Some authors have proposed that this
2 phenomenon is caused by the strong dependence of dissolution kinetics on local dissolved metal ion
3 concentration (e.g., [198]).

4
5 The present review found that only continuum models were available for propagation events.
6 Although these models are able to model pit propagation reasonably well (as it is a relatively higher
7 scale event), they can be applied only indirectly using empirical parameters that account for
8 associated mechanisms rather than explaining the direct influence of causal factors such as
9 microstructure. Thus, continuum models are not sufficiently general to be incorporated into a truly
10 generic MSM. Additionally, a deep understanding of electrode kinetics that would facilitate the
11 development of reliable atomistic models was lacking.

12 13 **4.7.1 Continuum models – the only option available**

14
15 Because the propagation mechanism is better understood than the nucleation mechanism, more
16 continuum models are available for pit or crevice propagation. Most models, including hybrid
17 versions, follow the deterministic path for propagation. However, a number of stochastic models also
18 exist. Sharland [62], Turnbull [214], Frankel [172], Scheiner and Hellmich [199], Kennell et al. [63],
19 Papavinasam [200] and Macdonald and Engelhardt [215] have reviewed traditional models and
20 formulations for propagation-related mechanisms, and only a selection of these models are reviewed
21 here from a multiscale modelling perspective. Stochastic models typically calculate expected values
22 of quantities such as the induction time or the number of stable pits as functions of defined parameters
23 such as the nucleation frequency, the survival probability and the critical age. Then, through the
24 interpretation of measured current transients, values for the parameters are retrieved. Stochastic
25 models of Williams et al. [36], Valor et al. [35], Alamilla and Sosa [33] are noteworthy examples.
26 While none of these models explicitly consider the microstructure, the previously mentioned
27 stochastic model for inter granular corrosion developed by Zhang et al. [68] (Section 4.1.1) utilised a
28 brick wall model with a rectangular 2D geometry for aluminium grains. This rather simplistic
29 description appears to be the closest stochastic approach published for modelling alloy microstructure.
30 To summarise, stochastic models have not explicitly accounted for critical factors. Rather, stochastic
31 models have relied on empirical parameters that were used subsequently to estimate various quantities
32 associated with propagation. Deterministic models invariably followed either the CSCT/CCST or the
33 RDT approaches. Often, early models (e.g., [160, 194-196, 202, 216, 217]) were developed for
34 idealised 1D geometries, supported only the steady state, and contained several simplifying
35 assumptions. Sharland and co-workers [30, 203, 218] and Engelhardt et al. [219] developed some
36 noteworthy models, but Walton et al. [183] appear to be the first to develop and validate a transient
37 model applicable to a wide variety of metals and electrolytes and supported by different kinetic rate
38 equations. Laycock and White [198] developed a 2D FEM model that successfully recreated the lacy
39 covers observed on pits on SSs. The deterministic model of Turnbull et al. [48] contained statistically
40 distributed parameters for the pit growth equation. When Laycock et al. applied the previously
41 developed propagation models [198] in their hybrid version [47], they accounted for different SS alloy
42 compositions by changing the OCP for each alloy and for surface roughness by altering the distance
43 of the initial spherical pit beneath the metal surface in the Tafel equation for anodic dissolution.
44 Additionally, the deterministic propagation equation in the hybrid model of Engelhardt and
45 Macdonald [46] for manganese steel in CO₂-acidified seawater and Al in tap water contains
46 empirically fitted parameters rather than values obtained from physical mechanisms. Such empirical
47 modelling has been carried out for Al alloy AA7075-T651 using neural networks by Cavanaugh et al.
48 [41]. Investigating two orientations of metal exposed to varying temperature, pH and [Cl⁻], those
49 workers concluded that pit growth generally followed $t^{1/3}$ kinetics. To summarise, most models used
50 the 1D approach to predict pit size and transfer processes [215], and existing continuum models of pit
51 propagation have not explicitly considered the effects of causal parameters such as alloy
52 microstructure, oxide films or surface roughness on propagation rates. Rather, these parameters have
53 been incorporated using quantities such as the OCP or the exchange current density (in the Butler-
54 Volmer equation, for instance) that were obtained empirically. The lack of generality makes it
55 difficult to use such models in an MSM for designing alloys or corrosion resistant systems.

4.7.2 Proposed improvements

There are very few atomistic models of pit propagation in the literature. The probable reasons for this situation are (a) the continuum models have tackled this phenomenon reasonably well on the continuum scale and/or (b) the computational cost does not justify applying atomistic simulations to phenomena on mesoscopic scales or continuum expanses. However, it is likely that atomistic methods will be used increasingly to simulate propagation and extend the boundaries of knowledge. There is a need for advancement in the fundamental theoretical understanding of electrode kinetics before reliable atomistic models can be developed. For instance, Macdonald and Engelhardt [215] recently noted that while Tafel constants may be calculated ab initio, the exchange current density is almost always measured experimentally because theory is not sufficiently developed to calculate this quantity from first principles. This is because Tafel constants contain relatively little kinetic information and the transfer coefficient is usually assumed to be 0.5 corresponding to a presumed symmetric barrier, whereas the exchange current density is derived from a highly kinetic and inherently complex set of mechanisms involving solvent reorganisation which are still poorly understood [220-222]. Once an understanding of the charge transfer reactions at the electrode/ electrolyte interface and related mechanisms is established on the atomic scale, however, rate equations such as Butler-Volmer or Tafel with empirically determined parameters to describe boundary conditions at the continuum scale will unnecessary. Recent phenomenological models [146] analyse charge transfer in solution in terms of a number of components and effectively refine the electrochemical scale. Lower scale models will manage the difficulties with mesh refinement on finer scales to better describe, for instance, small-scale material removal or large concentration gradients near the electrode/ electrolyte interface under diffusion control. In a nutshell, pit propagation can be modelled reasonably well on mesoscopic scales in the absence of a lower scale model. In this case, the incorporation of microstructural details at the electrode/electrolyte interface should be considered in the medium term. However, because the atomistic description gives the best resolution, efforts should be made to incorporate atomistic-scale models in advanced versions of the MSM. Development of such models may remain a challenge until issues with computational loads are resolved through hardware and/or software improvements. Finally, the potential use of mesh-free methods for pit propagation should also be explored because these methods are well suited for modelling moving discontinuities.

4.8 Changes in electrolyte chemistry in pits

The concentrations of species in a pit are affected by electrochemical reactions such as anodic dissolution and cathodic reduction at the electrode/ electrolyte boundary, chemical reactions such as precipitation (see Section 4.9) and dissolution of O_2 and CO_2 at the electrolyte/air boundary as well as dissociation and hydrolysis in the aqueous environment. As a pit grows and the pit depth exceeds the width of the pit mouth, diffusion is restricted between the confined localised pit volume and the bulk solution. This results in the depletion of consumed species (e.g., dissolved oxygen) in the pit but the enrichment of dissolved metal ions. Such enrichment results in the migration of anionic species such as Cl^- from the bulk to preserve electro-neutrality and the hydrolysis of the dissolved metal ions that releases H^+ ions in the pit and lowers the pH. This acidic chloride environment is aggressive to most metals and tends to prevent repassivation and promote pit propagation. Further information about this subject may be found elsewhere [57, 61, 223-226].

The current review established that the only models on the continuum scale were available, and the lack of resolution as well as simplifying assumptions limited the application of these models.

4.8.1 Continuum models – purely deterministic

Stochastic modelling of pitting is not commonplace. Sharland [62] reviewed some of the early studies and concluded that no single model predicted (qualitatively or quantitatively) all the available experimental observations. The Walton model [183] predicted concentration profiles more accurately than previous versions. Evitts [227] carried out an extensive review of both steady state and transient models that dealt with changes in chemistry, including the studies by Sharland [30, 203, 218] and Walton [183], and concluded that most models assumed isothermal conditions and constant bulk solution chemistry. Macdonald and Engelhardt [215] noted that most models are 1D and erroneously neglect the potential drop outside the corrosion cavity, leading to significant errors in the prediction of damage. The White et al. [228] model relied on the Nernst-Planck equation rather than the electro-neutrality condition for the calculation of potential differences and predicted concentration profiles for an SS system. Laycock and White [198] calculated the local chemistry in an SS pit and accounted for several relevant criteria including a moving boundary due to propagation. More recently, Kennell et al. [63] developed a combined CCST/CSCT-IRDT model that provided the best agreement yet with the experiments of Alavi and Cottis [229], surpassing the models of Sharland [218], Walton [183], White [228] and Evitts [227], and introduced the possibility that such a combined approach may be superior to the CCST/CSCT-only path. Taxen and Persson [230] considered concentration changes due to the evaporation of aqueous electrolyte and used a moving mesh, but the application of the dilute solution theory was discontinued beyond a certain loss of volume. Finally, Heppner et al. [231], noting that most models assumed a dilute solution, carried out theoretical calculations for non-ideal solutions where ionic interactions could no longer be neglected. Their work, which used the Pitzer model [232], simulated crevice corrosion evolution including species concentration changes and delivered better predictions than those models that did not account for ionic interactions. Thus, the use of the Pitzer model in the MSM should be explored, especially for non-ideal solutions. Moreover, in actual solutions, the activities of species can change not only with temperature but also with pH values [15]. Even for dilute solutions, traditional models relied on estimating activity coefficients from theoretical models (see [15],[183],[233]), and advanced modelling on this front should be considered. Another common feature in traditional modelling was the lack of data on chemical reaction kinetics. Therefore, several assumptions were made. For instance, Sharland and Tasker [218] assumed that the chemical reactions occurred at very high rates compared with other phenomena such as diffusion. While many such assumptions may be justified for continuum models, they are invalid for atomic scale models. To conclude, the existing models that describe chemical changes in a pit all belong to the continuum scale and thus lack detail on the mesoscopic scale for some relevant events discussed below.

4.8.2 Atomistic models – may be required for non-dilute solutions

Lower scale atomistic models that describe changes in solution chemistry are rare in the corrosion domain. This may be because the chemical changes are largely a response to other events rather than being causal events themselves. This means that, if events at electrolyte-electrode and electrolyte-air boundaries were modelled with sufficient accuracy and the important chemical reactions were properly accounted for, the chemical changes in the pit would be adequately modelled at the continuum scale without the need for a computationally intensive atomistic treatment. Nevertheless, as the theoretical work of Heppner et al. [231] showed, ionic interactions may become significant in non-dilute solutions where dilute solution theory would break down. Such cases might benefit from atomistic-level computations which can provide the necessary resolution to model the interactions in more detail. For instance, in the multiscale framework, an atomistic-scale model can be used to calculate the empirical parameters (e.g., the activity coefficients and the osmotic coefficient) for the Pitzer model [232] for deployment at a higher scale, although these parameters have been experimentally derived for some systems [234]. Furthermore, the following events may be better modelled at a scale lower than continuum: (a) the influences of alloy microstructure on local chemistry (e.g., through space-dependent dissolution) or vice versa (e.g., the local chemistry can preferentially attack metallurgical defects); (b) the passive film or its influence on the chemistry; (c) the microenvironment defined by the microscopic surface roughness; or (d) interactions between pit

1 sites. Such detail is desirable in an MSM that will be used in a predictive role in alloy design. MD
2 simulations of non-ideal solutions have been performed [235, 236], and perhaps similar studies could
3 be used to explore the concentrated solutions that develop in pits.
4

5 **4.8.3 Proposed improvements**

6
7 In non-dilute solutions, phenomena such as ionic interactions within the electrolyte may not be
8 neglected and ideally are modelled on the atomic scale to arrive at an optimum generic approach that
9 could be used widely. Another area that needs to be strengthened is the quantification of reaction rate
10 constants for some reactions. Although these constants could be obtained experimentally for some
11 reactions, other extremely rapid reactions present difficulties in the determination of rates because
12 reliable experimental measurements cannot be made easily using traditional methods [237]. In the
13 absence of dependable measurements, the application of theories such as [238] collision theory or
14 transition state theory may be attempted for estimating reaction rates, and subsequently rate constants
15 (see [239]). Alternatively, these may be obtained from the application of first principles (e.g., [19]).
16 Similarly, it appears that no current document has a comprehensive listing of all relevant parameters
17 such as those above and others such as dissociation constants and solubility products that a modeller
18 could conveniently access, although some handbooks contain samples of these. Therefore, there are
19 opportunities for developing atomistic models capable of estimating these quantities.
20
21

22 **4.9 Precipitation of corrosion products**

23
24 During localised corrosion, some salts precipitate on the corroding substrate as a result of reactions
25 between dissolved anions and species in the electrolyte in the pit or crevice (see, e.g., [85]).
26 Precipitation occurs when the product of the ionic reactants exceeds the solubility product. The
27 corrosive microenvironment under surface deposits is very different from the bulk solution. In
28 particular, the pH of these microenvironments tends to be very acidic. The formation of acidified
29 microenvironments is related to the hydrolysis of corrosion products and the formation of differential
30 aeration cells between the bulk environment and the region under the deposits [59]. Precipitation of
31 salts on electrode surfaces can affect the anodic and the cathodic reaction rates by modifying the
32 extent of the areas that are in contact with the electrolyte and/or increasing the resistance of the
33 passive film to charge transfer. For example, the dependence of the Zn corrosion rate on pH is
34 determined by the corrosion products [61]. Conditions controlling the thickness of products in zinc
35 [61] and SS [240] systems are discussed elsewhere. Given the rate-controlling nature of the
36 precipitates and the alterations to solution chemistry, an MSM should have the facility to adequately
37 account for corrosion products.
38

39 The present review found that only continuum scale models were available to address precipitation,
40 and these models contained sweeping assumptions such as homogeneous electrodes to describe what
41 are, in essence, atomistic phenomena that are influenced by the heterogeneous electrochemical
42 behaviour of electrode surfaces.
43

44 **4.9.1 Continuum models – severely lacking in detail, but the only type available**

45
46 As with the changes in pit chemistry (Section 4.8), only deterministic models are relevant for
47 describing precipitation. Models that account for precipitation include those of Gravano and Galvele
48 [196], Sharland and Tasker [218], Sharland [203], Walton et al. [183], Laycock et al. [25] and
49 Laycock and White [198]. These models provide different mathematical treatments of precipitation.
50 For instance, Gravano and Galvele [196] treated precipitating solids as colloidal diffusing species in
51 their work that focused on solution chemistry immediately after film breakdown. The 1D transient
52 model constructed by Sharland [203] was one of the first models to predict the evolution of solid
53 phases (corrosion products) as a function of time and space in addition to solution chemistry and

1 electric potential. All the above models assumed that the precipitation of the metal hydroxide occurred
2 when its concentration reached the saturation level in the solution; Laycock and White [198],
3 however, allowed up to 10% super-saturation to occur owing to their additional assumption that a
4 hydroxide salt film could precipitate only on an existing salt film or on the corroding metal. A slightly
5 different approach was followed by Taxen and Persson [230], who assumed that precipitation
6 occurred when the activity coefficient for any solid species in solution exceeded unity. Another aspect
7 of traditional modelling has been the limited use of data for rates of precipitation by many models
8 (e.g., [218]) based on the assumption that rates of precipitation are much higher than other events such
9 as diffusion. It was necessary to make these assumptions in the traditional models due to the general
10 lack of data on chemical kinetics and rates of precipitation [218], which has remained the case to this
11 day [215]. Some workers such as Farrow et al. [110] worked around this issue by using theory [241]
12 to estimate the rates. Some works such as Nescic and Lee [242], Sun and Nescic [243], Anderko [15]
13 and Taxen and Persson [230] dealt with the subject in the sphere of general, rather than localised,
14 corrosion. Also worthy of mention is the work of Tidbald et al. [244] who used the well-known
15 GILDES model [241] for atmospheric corrosion to predict the formation of corrosion products on
16 copper substrates exposed to aqueous species. The GILDES model solves the mathematically
17 formulated transformations and transitions that occur in the six relevant ‘regimes’: the gas phase, the
18 interface between a gas and a liquid, the liquid phase, the deposition layer, the electrode region near
19 the surface and the solid phase. With the exception of studies such as that of Farrow et al. [110] and
20 the GILDES model [241], none of these models have accounted for the well-known influence of
21 surface pH on precipitation by simulating the dissolution of precipitate layers in certain pH ranges –
22 so these models were limited to pH ranges where the products were stable. None of these models also
23 took into account the effect of microstructure and were unable to provide the details required to model
24 mixed corrosion products, such as different oxides of alloy components or their spatial distribution
25 that depends on microstructural features besides alloy composition. Additionally, none of these
26 models explicitly accounted for the passive films. Because the electrode was assumed to be
27 homogeneous on the macroscopic scale, the available models do not contain the details that a
28 prospective microscopic or lower-scale model would be capable of furnishing. Thus, the available
29 models need fine-tuning from the perspective of incorporating precipitation algorithms into an MSM.
30

31 **4.9.2 Proposed improvements**

32
33 The present authors did not find any atomistic scale models that dealt with corrosion products,
34 although, like oxides films (Section 4.2), the usually ultrathin and porous nature of precipitate layers
35 make them classic examples of why a multiscale-approach should be taken for modelling localised
36 corrosion. The atomistic scale provides the ideal framework for modelling transport at not only the
37 interfaces between the products and other components such as the passive film or the metal itself but
38 also through the products themselves. This is also the most suitable method for modelling interactions
39 between the electrolyte and the products including adsorption. In addition, bonding at interfaces may
40 be modelled elegantly using an atomistic approach. Thus, there is scope for building models of
41 corrosion products at the lowest scales in the medium to long term. These models should take into
42 account the microstructural inhomogeneity of the metal substrate and the oxide when predicting the
43 space-dependent structure and thickness of the precipitate layers. It may be possible to develop
44 atomistic precipitation models for corrosion based on precipitation kinetics-related models that are
45 becoming available in other fields, e.g., solidification - atomistic [78] and hybrid atomistic-kMC
46 [245]. Additionally, the inverse of precipitation (dissolution) of salt films has been studied recently
47 using MD [246], and this approach may be examined for developing a basis for precipitation models
48 of corrosion.
49
50

1

2 **4.10 Repassivation**

3

4 Under certain circumstances, the increasing corrosion partial current that follows a nucleation event
5 may cease. This is attributable to repassivation and is due to the loss of the active surface on the
6 electrode. Despite the autocatalytic nature of pitting, even large pits can stop growing or die [57].
7 Whilst the repassivation of the corroding surface stifles the growth of pits, the increasing ohmic
8 potential drop along the depth of the pit also results in the pit being stable at a low anodic current
9 density at the bottom. That is because, as the pit deepens, the diffusion of the cations out of the pit
10 reduces - thus decreasing the rate at which these ions dissolve from the substrate. At some point, the
11 pit stops growing and is considered 'dead'. The repassivation mechanism/s for metastable pits are not
12 known for certain [247]. Relatively recent high-resolution experimental works, however, are
13 beginning to illuminate some of the mechanisms involved in repassivation. For instance,
14 Chidambaram et al. [248] have observed, through synchrotron infrared microspectroscopy and
15 secondary ion mass spectroscopy, that the slow migration of ions from the surface of AA2024-T3
16 alloy protected by chromate conversion coatings to the scratch-exposed metal surfaces leads to the
17 repassivation of the metal. A similar mechanism might be operating in metals protected by oxide
18 films. Furthermore, the quantitative effects of the alloying elements on kinetics have been studied by
19 some workers. For example, Cho et al. [249] have quantified the influence of alloying elements on
20 repassivation kinetics. Data on repassivation kinetics remains scarce. However, repassivation kinetics
21 are considered to be a critical factor in determining the resistance of metals and alloys to localised
22 corrosion [250] and, consequently, in influencing the accumulated damage [104]. Thus, there is little
23 doubt that any MSM built for use in the design of corrosion resistant alloys should be able to simulate
24 phenomena relating to repassivation.

25

26 This review found mostly continuum scale models that relied on Pourbaix diagrams for equilibrium
27 conditions and mostly empirical data for non-equilibrium situations – and thus had little general
28 applicability. This review also highlighted the lack of atomistic models and experimental data on the
29 smaller scales.

30

31 **4.10.1 Continuum models – inadequate**

32

33 Traditionally, conditions under which repassivation occurs have been determined by the use of
34 Pourbaix diagrams [247]. However, this phenomenon has been addressed by a handful of empirical
35 and continuum mathematical models as engineering situations deviate significantly from the
36 equilibrium-based scenarios. Examples of empirical models include that of Song et al. [251].
37 However, as the empirical models do not explicitly incorporate the influence of, for instance, the
38 environment or material properties, they cannot be utilised as generic tools. Stochastic modelling
39 works have attempted to incorporate the repassivation phenomenon using probabilities. For example,
40 in the model by Williams [36] an assumption regarding the probability that a metastable pit will
41 repassivate was made. However, these stochastic models – like their empirical counterparts – do not
42 explicitly account for mechanisms leading to repassivation. Among deterministic models, the Walton
43 et al. model [183] appears to be the first that is capable of simulating repassivation, as it supported the
44 active/passive transition. Laycock et al. [25] assumed that repassivation would occur if the diffusion
45 of metal ions away from the electrode exceeds their production through dissolution, in which case the
46 ion concentration tends to zero. Anderko et al. [252, 253] developed mechanistic models based on
47 statistical thermodynamics. Their models calculated the repassivation potential for selected SS and
48 Ni-base alloys whilst accounting for the influence of solution chemistry (aggressive species,
49 oxyanions and inhibitors), temperature, competitive dissolution, adsorption and oxide formation. In
50 particular, the models predicted the transition from the concentration range where localised corrosion
51 was favoured to the region where inhibition was expected. Some of the parameters in the Anderko
52 models [252, 253] were experimentally obtained. A PDM [26, 104, 215] was capable of explaining
53 the experimental observations of Ahn et al. [254] for the repassivation kinetics of Ti. However, as

1 noted by Wu and Celis [255], HFM is the most widely used explanation of repassivation kinetics,
2 although its validity has been questioned by some. Whilst some experimental works (e.g., [255-257])
3 have supported the application of HFM, Wu and Celis [255] caution that HFM may not be physically
4 realistic at very short times following depassivation. To summarise, while continuum scale models
5 exist, they are inadequate for modelling repassivation because it is known that lower scale factors
6 influence this phenomenon. For instance, second phase particles or inclusions in an engineering alloy
7 would exhibit electrochemical potentials different from that of the matrix – and can preferentially
8 passivate (or dissolve). Such resolution at the microscopic level is mandatory for an MSM aimed at
9 alloy design.

11 **4.10.2 Atomistic models and experimental data at this scale are scarce**

13 Using Monte Carlo simulations, Malki and Baroux [185] determined that varying the repassivation
14 probability on the atomic scale on the pit walls can control pit growth kinetics (t^n law), but the authors
15 admitted that there was no experimental evidence to suggest that this unexpected prediction was
16 tenable. This model appeared to be the only one in the open literature that dealt with repassivation,
17 and the lack of models at this scale is probably explained by the scarcity of experimental data on this
18 scale. However, atomistic simulations have been performed for the oxidation of metal surfaces, which
19 is a critical step in repassivation – e.g., MD simulations by Sankaranarayanan [258] and DFT work by
20 Schröder [258]. Perhaps strategies found in these works can be applied to develop a model for
21 repassivation.

23 **4.10.3 Proposed improvements**

25 More experimental observations on the atomic scale are required to understand the mechanisms that
26 lead to repassivation in situations that do not involve the preferential dissolution of phases or
27 inclusions. It therefore stands to reason that atomistic scale models will be the most appropriate means
28 to describe such phenomena. However, the existing models that account for repassivation have all
29 been developed on the macroscopic scale. Additionally, no existing model has taken into account the
30 role of the microstructure, for instance in the apparent repassivation of pits formed by selective
31 dissolution. It is also necessary to determine through experimentation whether the presence of
32 different phases or other microstructural features in the local neighbourhood would have any
33 influence on whether a pit repassivates. Such influences may be modelled at the microscopic level and
34 will enrich an MSM designed for alloy design.

37 **4.11 Interactions with the immediate neighbourhood**

39 A passive surface exposed to an aggressive corrosive environment is usually riddled with numerous
40 pits. Due to a competitive interaction process between these pits, only the strongest survive to grow
41 [104, 259]. A stronger pit, which generates a higher current, competes for a larger share of the
42 charged species by attempting to expand its “living space” - the volume of electrolyte immediately
43 adjacent to the pit. The stronger pit thus suppresses its weaker neighbours. In some cases, possibly
44 when the competing pits are similar in strength, they coalesce. Recent high-resolution experimental
45 observations [169, 170] have suggested that an autocatalytic explosion of metastable pits may be
46 possible, at least in SSs. Therefore, it is useful to reproduce these interactions in detail in an MSM so
47 that corrosion sites are predicted realistically.

49 Despite the dominant influence of the electrochemical properties of the *microenvironment*
50 surrounding a pit on determining the favoured interactions (which calls for lower-scale modelling),
51 only continuum models were found during the present review. With greater understanding of pitting at
52 the lower scales, it should be possible to model these interactions at the atomic level.

4.11.1 Continuum models – hybrid treatment

Only a handful of existing models address this topic, and this is probably due to (a) the lack of experimental data and associated understanding, which is only just beginning to filter into the open literature, and/or (b) the probable perception that such interactions may only be of secondary importance. Available models generally take a hybrid approach treating nucleation and interaction events stochastically but employing deterministic equations for the influence of the environment. One of the first models that accounted for interactions was the previously mentioned stochastic model of Wu et al. [37], in which a memory parameter, M , was incorporated to retain the influence of a given event over time. Lunt et al. [260] extended this model and their simulation results, which agreed with experimental data obtained by the same workers on an array of SS electrodes, showed that surface damage gave the highest M value. Organ et al. [182] extended the Lunt et al. model to 2D, and this model suggested that interactions among metastable pitting events can lead to the formation of clusters of pits. White et al. [261] developed an FEM model incorporating interactions as an extension of a previously discussed model by Laycock et al. [47]. Their model confirmed that an existing pit would increase the probability of pits nucleating at nearby sites. Harlow and Wei [262] developed a stochastic model incorporating interactions for pit growth in Al alloys. Although not validated with experiments, the authors mentioned that its predictions were in qualitative agreement with observations. Significantly, the authors advocated a deterministic approach for a more realistic analysis of interactions. A mechanism of competitive interaction between pits at the early stage of their development was considered by Popov [259], who assumed that the interaction occurred due to the hydration of metal ions by the solvent. Popov derived analytical equations and proposed a 1D model of interaction between two linearly connected pits. However, this model was not validated with experimental data.

4.11.2 Proposed improvements

Only a limited number of models have addressed the phenomenon of interactions between pits. All of these models were on the continuum scale, and the electrode surface was modelled as homogeneous, without preferred nucleation sites. Therefore, a stochastic approach was followed for nucleation events, and interactions were modelled by deterministic equations that incorporated the influence of the environment on interactions. Clearly, the assumption of homogeneity reduces the detail required in a model for alloy design. Therefore, a model at the mesoscopic scale should be developed for describing the interactions on their characteristic scales. It would be an advantage to have an atomic scale model to describe nucleation events. However, limitations of atomistic models addressed earlier in section 4.4.3 with respect to non-equilibrium events must be adequately dealt with before dynamic processes such as interactions can be realistically modelled at that scale. In addition, although recent in situ experiments and modelling indicate that an existing pit would increase the likelihood of pits nucleating at adjacent sites – at least on SS, it would be desirable to have additional observations of different corrosion systems. Lastly, when more experimental data becomes available, replacement of the stochastic treatment by deterministic mechanisms would help interrogate the models and thereby increase our understanding of the controlling factors.

4.12 Summary

Fig. 5 provides a summary of approaches discussed in some detail in the preceding sections. Continuum approaches are shaded in red and atomistic in green.



Figure 5: A summary of approaches found in the literature for the various events relevant to localised corrosion. Continuum approaches are shaded in red and atomistic in green.

5.0 Numerical strategies

In this Section, issues unique to the solution of equations on multiple length and time scales are addressed.

5.1 Field variables at different scales

The primary challenges for modelling corrosion where different scales of time and length are linked can be classified broadly as *formulational* and *computational*. Formulational challenges arise when two or more apparently dissimilar modelling philosophies operating at different scales are combined to explain a phenomenon such as corrosion. It is a formidable task to combine the mathematical structure of one modelling approach with another while ensuring a seamless information exchange between the different models. Computational challenges, on the other hand, include appropriate hardware, efficient multithreaded parallel programming, approximation and fault tolerance, data visualisation and data transfer between various computing units. In this section, we concern ourselves primarily with formulational challenges of multiscale modelling and some computational challenges inherent in the development of an MSM for corrosion.

The central difficulty in coupling two methods on different scales is reconciling the definitions of computational variables. Two quantities are of primary interest: the total energy of the system and the temperature. The standard approach is to construct a potential energy functional and use its derivatives to obtain the forces necessary to evolve the system. However, Curtin et al. [263] note that the fundamental problem in bridging the continuum and atomistic methods stems from the fact that the expressions for the total energy of the system are fundamentally different in the two methods. They observe that apart from the semi-empirical nature of the interatomic potentials employed in MD, which introduce uncertainty and approximations, the quantum energy, unlike its classical counterpart, cannot be partitioned into energies on a per-atom basis. This was reiterated by Makov et al. [264] who observed that, in the case of an MSM, two potential Hamiltonian formulations could be used for the atomistic and the continuum models. When more than one model Hamiltonian is used, it is normally assumed that the energies in the system are additive. However, the additivity of the energy is scale-dependent, being valid at large scales (continuum) and invalid at short scales (atomistic) due to the existence of long-range interactions and quantum non-locality. Thus, the width of the boundary zone where the models "shake hands" must be chosen such that no forces are introduced artificially. Makov et al. [264] have described a "Learn on the Fly" (LOTF) multiscale approach in which the entire system is represented in the high level, and the region of the low level simulation is determined dynamically (i.e., continuously updated) by flagging the 'quantum' atoms according to a mixture of topological (bonding lengths and angles) and geometric (e.g., distance from the crack tip) conditions. The potential used to derive the forces in the boundary zone is fitted to the results of the low-level atomistic simulation, and this unique potential describes and conserves momentum.

On the other hand, Ganzenmuller et al. [265] observe that both the heat flux and the temperature are interpreted differently in continuum and atomistic domains. The continuum approach is based on discretising a continuous field of state variables at discrete spatial locations. The momentum, mass (and species), charge and heat fluxes are then evaluated between these nodal points. Many techniques including Finite Difference [266], FE [267], Control Volume [268] and their hybrid variants [269] employ this scheme. Techniques such as Smoothed Particle Hydrodynamics (SPH) [56] based on Lagrangian methods, where the evolution equations are not constrained by the need to track the movement of the fluid particles, also evaluate the fluxes using averaging techniques similar to the earlier methods. Molecular properties such as viscosity (internal friction) are usually provided as transport parameters to the simulations. The conservation equations usually are developed for mass (species), energy, momentum and charge separately and solved by effectively capturing the non-linear coupling between the variables. However, in MD, the kinetic energy of the interacting atoms depends on the

1 momentum exchange because no other degrees of freedom except those associated with the particle
2 kinetic energy are present and, thus, the temperature depends solely on the momentum. Ganznemuller
3 et al. [265] christen the average temperature in MD simulations as the *kinetic temperature* because it
4 stems purely from the kinetic consideration of a large number of interacting atoms. They distinguish
5 this from the *continuum temperature*, which in continuum models is defined using the concept of
6 internal energy and heat capacity. They further assert that the kinetic temperature in an atomistic
7 simulation relates to the average particle momentum, whereas the continuum temperature (even if
8 coupled to the momentum conservation equation) serves only as a *state variable* without any relation
9 to the momentum of the corresponding continuum integration node. Ganzenmuller et al. [265] further
10 observe that a correct continuum-MD coupling algorithm must describe the heat flux between the two
11 domains such that the continuum variable internal energy is linked locally to the MD particle velocity.
12 They also advocate Dissipative Particle Dynamics at constant Energy (DPDE) as an ideal choice for the
13 mesoscale coupling. DPDE, albeit an isothermal method, has provisions for assigning an “internal
14 temperature” to each particle that can be related directly to the internal energy and the heat capacity,
15 and the local DPDE thermostat is used in the MD domain to achieve dynamic equilibrium between both
16 temperature definitions.
17

18 **5.2 Modelling electric potential**

19
20 Another closely related issue is the “conjugate problem” [269] in which two or more regions (or phases)
21 are involved and there is a “jump discontinuity” in the material properties and state variables. In
22 corrosion, we encounter two or more phases where some quantities must be defined unambiguously to
23 ensure continuity. Electric potential is the only macroscopic variable that is present in both the solid
24 and the solution domains, although a discontinuity is prescribed (i.e., the potential of the metal and the
25 potential of electrolyte have different values) at the solid-solution boundary to quantify the
26 electrochemical surface reaction using Butler-Volmer kinetics. The reason for these discontinuities is
27 simply the incapability of the continuum models to describe atomistic details. In the continuum
28 methods such as the Control-Volume Finite Element method (CVFEM), the mesh is constructed such
29 that any given integration element falls in one and only one region, which ensures there is no ambiguity
30 in calculating the face diffusivities in a given element. While the conjugate problem is based on a
31 genuine phase-differentiation, the atomistic-continuum boundary zone is only a *numerical artefact*.
32 Thus, while it is important to ensure that modelling the conjugate problem considers accommodating
33 the atomistic details of the interface, it is equally important to ensure that the spurious forces at the
34 “numerically created boundary zone” do not contribute to the atomistic-continuum handshaking as well.
35

36 **5.3 Candidates for future MSM and mathematical coupling of scales**

37
38 Tan [12], Elliott [5] and Curtin et al. [263] have reviewed a number of multiscale methods with
39 particular emphasis on fracture. Tan discussed stress-corrosion cracking and pitting corrosion and
40 observed that stress corrosion cracking is the result of sufficiently strong mechanical forces that separate
41 chemically bonded atoms and also presented a case where hydrogen interacted with dislocations.
42 However, the combined interaction of mechanical stress (developed due to deformation or loss of
43 atoms) and electrochemical reactions underlying corrosion was not discussed in detail. Similarly, Tan
44 discussed pitting corrosion in the context of Monte-Carlo simulations performed by Reigada et al. [32],
45 who assumed that the probability of “tunnelling” (metal oxidation) depended linearly on the local halide
46 concentration and exponentially on the applied potential. Bartosik et al. [270] considered that pit
47 nucleation is a rare event at the atomic scale and that a Monte-Carlo simulation is still far too large for
48 currently available computational resources. They also noted that the complicated spatial and temporal
49 oscillatory behaviour exhibited by metals undergoing passivation in solutions poses a strong challenge
50 to the development of a unified approach for covering various aspects of corrosion. Thus, at the
51 mesoscopic scale, they have proposed a CA model that is characterised by seven species: metal M,
52 reactive site R, passive site P, electrolyte E, anodic dissolution site A, and cathodic site B. They

1 enforced local rules and noted the interdependence of the A and the B sites and the underlying
2 connectivity in the metal matrix that ensures that the electrons lost at an A site are compensated exactly
3 and simultaneously at a B site. CA methods on mesoscales typically require huge grids, and establishing
4 a connected path in the metal matrix for three-dimensional simulations is very time-consuming. This
5 method, although in an early stage of development, shows promise for future MSM applications because
6 it is one of the very few methods that accounts for global charge conservation, which is a stringent
7 requirement for corrosion. This approach however has not yet accounted for the following phenomena:
8 a) the diffusion and migration of species such as dissolved oxygen in the electrolyte, which determines
9 local corrosion rates; b) the effect of metallic microstructure including local phase compositions on
10 multi-phase/ polycrystalline metals and/or alloys; c) distributions of defects in the microstructure; and
11 d) effects of porous semi-conducting oxides (precipitated from the solution or natively formed) that
12 affect the permeability/ percolation of the electrolyte and host oxygen reduction reaction on their
13 surfaces [271, 272], thus enhancing corrosion rates to more than expected levels for metals such as iron
14 and zinc. The CA models can be refined to an atomistic level and the atomistic-mesoscale
15 coupling can be achieved by refining the cells to match the atomistic surface morphology. This
16 refinement could place a high computational load on the current CA models especially for corrosion on
17 a contiguous metal surface. The CA models could be combined with control-volume from CVFEM
18 techniques, which will account for reactions and ionic movement in the solution phase. Additionally,
19 SPH is another method that can include localised precipitation [273]

20
21 Elliot [5] observed that the atomistic-mesoscale coupling can be performed by ‘coarse-graining’ at the
22 boundary-zones and integrating out redundant degrees of freedom. This is achieved either by forcing
23 atoms onto a lattice or by grouping them into larger particles. The Lattice Material Point Method
24 (LMPM) [12] or SPH [56] could be used for this purpose. In both LMPM and SPH, the continuum
25 material point is modelled as an aggregate of atoms (“particles” or “atomic aggregates”), and the entire
26 continuum is modelled as a collection of material points (or particles) although, unlike SPH in LMPM,
27 a background mesh is always used. In both methods, a Lagrangian description is used to discretise the
28 material into a collection of atoms whose motions characterise the deformation of the material. In
29 LMPM, once the atoms are combined into larger particles, a quadtree or octtree method could be
30 systematically employed to aggregate the atoms in the transition zone for 2-D and 3-D models,
31 respectively. The stresses are calculated from velocities that are computed using Verlet algorithms
32 [274]. However, Hoover [275] warned that the analogy linking the SPH to atomistic MD also suggests
33 that the SPH representation of a continuum might exhibit the same chaotic instabilities that are present
34 in atomistic systems. Ganznemuller et al. [265] proposed a coupling strategy wherein they employed
35 SPH for the partial differential equations in the continuum to which a region with atomistic length-
36 scales and corresponding particle dynamics was coupled and this region was described by classical MD
37 employing a DPDE thermostat. Interpolations could help damp some of the oscillations encountered at
38 the boundary points, but LMPM, although computationally expensive, seamlessly integrates with the
39 framework of MD.

40
41 There is another interesting issue, mentioned briefly in sections 4.4.3 and 4.11.2, which requires
42 discussion. It concerns with the difficulty of linking electron transfers during non-equilibrium
43 situations such as the formation of anode and cathode at the atomistic scale, where calculations are
44 typically carried out for equilibrium configurations. As previously indicated (section 4.4.3),
45 fluctuation theorems [165] may provide a pathway for dealing with such events because they enable
46 quantitative predictions on fluctuations in small systems that are monitored over short periods to be
47 made; therefore the fluctuation theorems allow thermodynamic concepts to be extended to apply to
48 finite systems. They describe the statistical fluctuations in time-averaged properties of many-particle
49 systems such as fluids driven to non-equilibrium states and provide some of the few analytical
50 expressions that describe non-equilibrium states. Incorporating the fluctuation theorems in the MD
51 simulations (which are formulated using a Newtonian approach and not using DFT) could provide a
52 method to predict the evolution of time-irreversible electrochemical systems of molecular dimensions.
53 Once these modifications have been incorporated, one could expect an electronic/ charge distribution
54 (thus non-equilibrium) to result from the calculations and subsequently the atomistic-mesoscale

1 coupling could be done by ‘coarse-graining’ at the boundary-zone by integrating out redundant
2 degrees of freedom using LMPM.

3
4 Another problem that requires consideration is solving equations on different scales. Consider that
5 anodic half-cell reactions constituting localised corrosion start at microscopic anodic sites and
6 eventually spread on macroscopic scales. Often, the microscopic anodic sites couple to much larger
7 cathodic areas on the continuum scale. Similarly, there is a vast difference in characteristic time scales
8 between (a) the almost instantaneous phenomena such as electromigration, chemical reactions and
9 electrochemical reactions; and (b) the decidedly slow processes such as diffusion. The partial
10 differential equations in an MSM that describe such incongruent phenomena occurring over different
11 length and time scales that are several orders of magnitude apart present numerical solution issues that
12 are known as stiff problems. A stiff equation is a differential equation for which certain numerical
13 methods for solving the equation are numerically unstable unless the step size is extremely small. The
14 main reason for this issue is that the equation includes some terms that can lead to rapid variation in the
15 solution. While generic solution strategies have been contrived to solve such problems, a complex set
16 of equations, as in the case of corrosion modelling, requires a customised approach to obtain a stable
17 numerical solution in a reasonable time frame. Developing such a successful solution strategy is part of
18 developing an MSM. Incidentally, Macdonald and Engelhardt [215] have discussed alternative
19 approaches to solving the system of equations containing chemical reaction and transport terms with
20 vastly different characteristic time scales and thereby rates also. The numerical method employed by
21 White et al. [228] separated concentration changes due to chemical reactions, which can have infinitely
22 large rates of change, from concentration changes caused by transport so that the partial differential
23 equations (PDEs) may be solved more easily. Walton et al. [183] and Sharland [203] decoupled
24 equations for precipitation reactions from mass transport and corrosion equations on the basis of vastly
25 different characteristic time scales. They used the same procedure when modelling changes in chemistry
26 inside the pit. Thus, in addition to overcoming the formulational challenges associated with the linking
27 of spatial scales, an MSM developer will need to resolve issues related to the different temporal scales.
28 In the latter, the coupled equations will need to be solved using techniques that account for: (a) properly
29 reconciled definitions of the computing variables (e.g., kinetic and continuum temperature), (b) stiffness
30 and (c) instabilities that may propagate from the lower scales to the higher.

6.0 Some suggestions on the features of a future MSM

Initial versions of MSMs on localised corrosion will have incremental improvements over current techniques rather than satisfying all of the lofty goals outlined in Sections 4.0 and 5.0 and will address only some of the fundamental challenges outlined therein. An enormous amount of modelling and experimental effort will be needed to develop an ideal MSM as envisaged here that will be generic enough to apply to different alloy systems.

Modellers will first need to decide whether their MSM will need to be a 3-scale model (e.g., [10]) or a 2-scale version (e.g., [75]). That decision will hinge on the degree of resolution sought at the various levels and will be dictated by project goals. As argued in Section 4.0, a realistic MSM for the development of corrosion-resistant alloys and inhibitors should be coupled to an MSM on alloy solidification. It appears that a parallel framework (Fig. 2 and [9]) is the most suitable option for this coupling as shown in Fig. 6 for a hypothetical case.

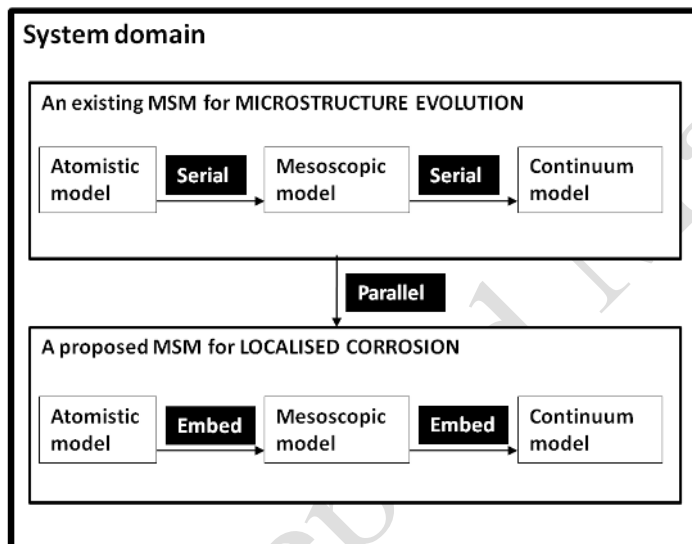


Figure 6: The different classes of integrating multiscale frameworks proposed for a hypothetical case where an existing MSM for microstructure evolution is coupled with a proposed MSM for localised corrosion.

As shown in Fig. 6, we favour an embedded framework (Fig. 2 and [9]) for an MSM on localised corrosion. This approach will reduce the overall computational burden by limiting the volumes computed at the lower scales. A rather detailed conceptual MSM on localised corrosion envisioned by the present authors is presented in Fig. 7.

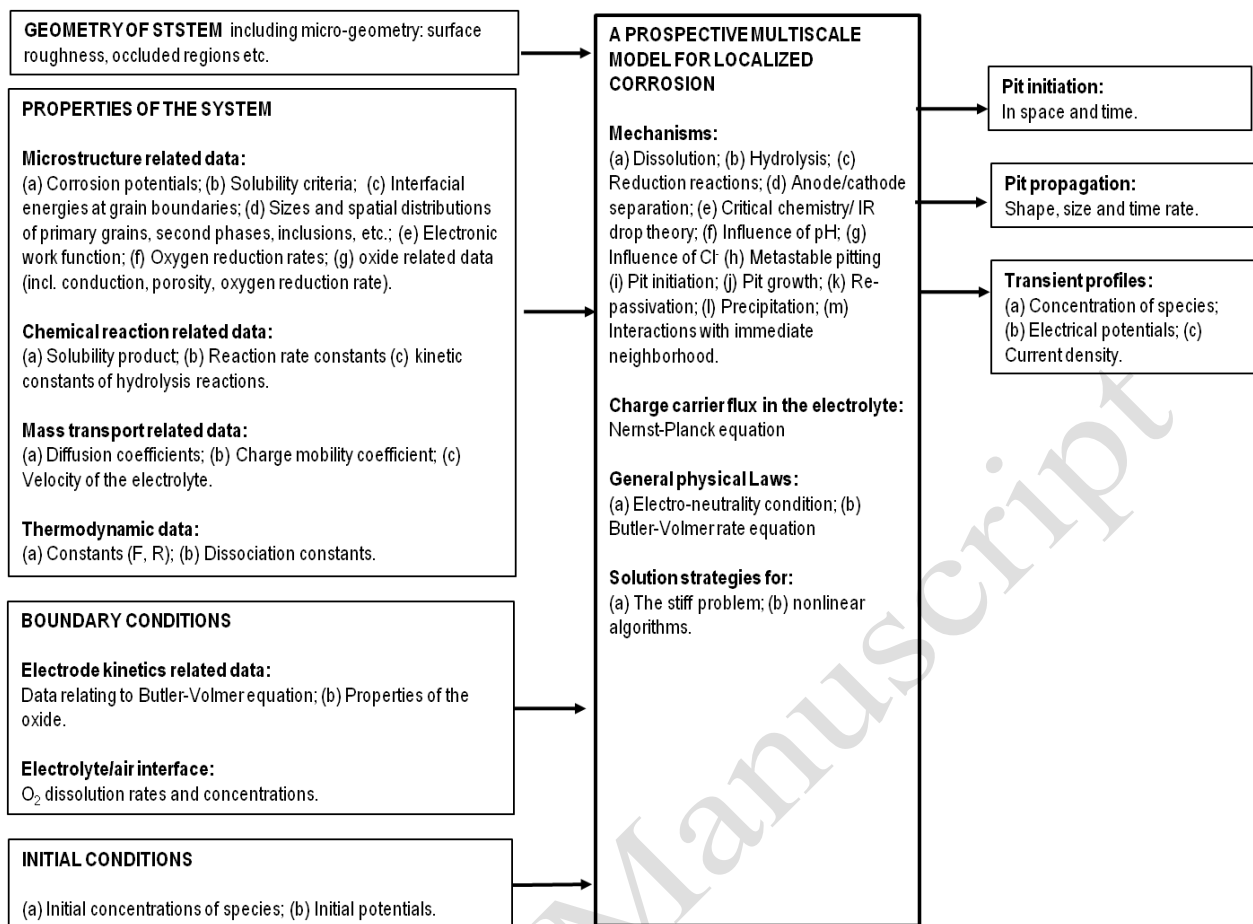


Figure 7: A general description of a prospective MSM on localised corrosion including potential inputs and outputs.

In developing a barebones MSM for corrosion, the following processes must be envisaged:

1. Metal oxidation
2. Metal ion dissolution, diffusion, speciation and hydrolysis
3. Oxygen reduction
4. OH⁻ ion dissolution, diffusion and further solution reactions
5. Precipitation of corrosion products from the solution
6. Effect of initial oxide layer
7. Solution Chemistry (migration and diffusion of other ions like Cl⁻ and inhibitors)

The favourable attack sites for corrosion on the metal surface are the defects and the grain boundaries. Hence, while developing an MSM for corrosion, it is imperative to model the surface atomistically using lattice techniques. However, unlike fracture, corrosion is basically a surface phenomenon that could potentially, in the long run, lead to a situation where the pits or crevices are large enough to cause material failure. Although apparently coupled, in the first version of the MSM we can delink the modelling of the electrochemical reactions from the modelling of material failure due to crack growth (which can be handled efficiently by many methods proposed in the literature [12] such as LMPM and the Quasi continuum method). Instead, corrosion modelling could concentrate on the interface and the large surface area over which pits initiate, grow, interact, stay metastable and/or die. However, the surface of most active metals is covered by an initial oxide layer, and localised corrosion occurs when this oxide layer is damaged. The PDM [26, 276], in principle, addresses defects and has a subtle connection with MD methods in the solid phase, although the PDM treats defects in a macrohomogenous fashion. While it is tempting to argue that the PDM or its variant [276] can

1 contribute to coupling algorithms, the connection between vacancy density and atomistic vacancies
2 needs to be established through conservation principles. On the other hand, the interaction of an
3 inhibitor with the metal surface is a vast subject that is currently gaining momentum [126]. While DFT
4 methods have been employed primarily to understand how inhibitors interact with metal surfaces in
5 solvated environments, the computational constraints dictate that this interaction, once well understood,
6 must be only semi-empirically accounted for using MD methods that can later be coupled with one of
7 the candidate continuum methods (FEM, CVFEM, SPH or LMPM) and mesoscale methods (CA and
8 DPDE) described above.
9

10 **6.1 Reactions**

11
12 At an international workshop [13] attended by eminent electrochemists, it was concluded that
13 progress in deterministic modelling will depend critically on progress made in the understanding of
14 the reaction kinetics of crucial corrosion reactions, although specific reactions were not identified.
15 The present authors discussed this in some detail in section 4.7.2. The workshop mentioned also
16 identified (i) a chasm between fundamental studies that focus primarily on ideal surfaces; (ii) the
17 challenges associated with real surfaces such as surface defects, surface films, adsorbed species and
18 water molecules; and (iii) a lack of knowledge about the morphology and composition of porous films
19 and the influence of alloying elements on film properties. Such knowledge is now beginning to appear
20 in the literature thanks to state-of-the-art experimental techniques, e.g., in situ electrochemical
21 scanning tunnelling microscopy [103], which sheds light on the initiation of nano-scale pits on nickel
22 surfaces.
23

24 **6.2 Mass transport**

25
26 It may be convenient to use the dilute solution theory [277] for the initial versions of the MSM,
27 although this is not recommended for real solutions. Activity coefficients that account for the non-
28 ideal behaviour of charged species at non-dilute concentrations should be used where possible.
29
30

31 **6.3 Micro Climate**

32
33 As outlined in Fig. 1, the lower level and pitting models will need to be connected to models that can
34 predict the “state” of the exposed surface where local attack occurs. By state, we refer to the presence
35 or absence of moisture, the chemistry of aqueous phases, and the temperature of the metal surface.
36 The models derived by Cole et al.[278-281] that link surface state to climate parameters and sources
37 and distribution of pollutants can be used or adapted for this purpose.
38

7.0 Conclusions

This review has highlighted both the complexity of developing MSMs and the possibility that a first generation MSM for localised corrosion that spans from molecular to component scales may be developed in the not-so-distant future. This MSM will have great utility for design, as it will allow the effects of atomic scale changes on the component performance to be determined. Thus, the molecular design can be optimised. Furthermore, processes that lead to the most rapid deterioration can be focused upon at their characteristic scales for additional research or development.

Current design approaches are based on continuum models. We outlined how these models were based on assumptions of homogeneity and were consequently limited for applications to heterogeneous materials and processes that require a heterogeneous description. This was most evident in the cases of material heterogeneity, such as complex multi-phase microstructures, oxide films, paint films and corrosion products. Most present models assumed homogeneous properties for the material units. Where limited heterogeneity was permitted, it was introduced by linking two homogeneous units and ignoring the boundaries. An example is the application of the porous electrode theory to model corrosion processes where the solid-fluid boundary was accounted for by superposing continua. On the contrary, molecular or atomic modelling in MSM will allow heterogeneities to be studied directly without the overbearing assumption of sweeping homogeneity, but at the same making necessary allowances for information exchange at the “handshake” regions where the continuum and discrete models intersect. For example, percolative transport of fluid through the oxide pores and its subsequent interaction with the metal surface underneath is a strong candidate where percolation could be modelled using statistical considerations (i.e., partially disregarding the discreteness in the distribution), and the reaction of the fluid with the metal surface could be modelled by DFT or MD techniques. As in the case of material structure, atomistic and molecular modelling can examine specific interactions between atoms and molecules that can then be linked back into a continuum scheme.

There are, however, significant challenges to developing a multiscale model. These challenges include:

- a) The overall formulation of the model so that processes and structures are modelled on appropriate scales;
- b) The development of models at each scale that are computationally efficient and provide results of appropriate accuracy and resolution;
- c) The linking of models on different scales in a computationally efficient manner, and
- d) The validation of the model overall and at each level.

This paper described a structure in terms of overall formulation and presented a number of possible approaches to this problem. The main computational costs occur on the atomic or molecular scale. As outlined by Elliot [5], efficient methods are required to accelerate molecular modelling and effective partitioning, and linking molecular and higher-level scales may be part of the solution. The exact method to link different scales probably will depend on the particular material and processes involved, and thus a tool-box rather than a prescriptive approach may be best. As discussed in Section 4.3.2.4, a “nano-gap” still exists between molecular modelling and continuum modelling of inhibitor effects. Addressing this gap is essential because most of the observed electrochemical phenomena depend on the double-layer properties. We discussed some of these strategies for linking DFT and MD to expand the fine scale or developing phenomenological models of electrochemical processes supplemented by refined measurements to model finer scales. Lastly, the validation of the MSM will be critical at each scale and at the overall model level. We emphasise that more refined experimental techniques will be required for this purpose.

Acknowledgements

The authors thank Prof. Rudy G. Buchheit (Fontana Corrosion Center, Ohio State University) who generously contributed to several discussions on topics of interest during his visit that was supported by a Fellowship from CSIRO and provided feedback on this manuscript. In addition, the authors would like to thank Dr. Michael Breedon (CSIRO) for discussions on molecular modelling and DFT. Highly useful suggestions were provided by Drs. Tony Cook (Manchester University) and Anton Kokalj (Jožef Stefan Institute) during their tenures as visiting scientists with CSIRO. This project was sponsored by the Advanced Materials Transformational Capability Platform (AMTCP) of CSIRO.

Accepted Manuscript

1

2 **References**

3 [1] M. Kutz, Handbook of Environmental Degradation of Materials, in, William Andrew, Inc., Norwich,
4 NY, 2005.

5 [2] Z. Ahmed, Principles of Corrosion Engineering and Corrosion Control, Butterworth-Heinemann,
6 Oxford UK, 2006.

7 [3] S. Zhang, Building from the bottom up, Materials Today, (2003) 20-27.

8 [4] N.S. Azmat, K.D. Ralston, T.H. Muster, B.C. Muddle, I.S. Cole, A high-throughput test methodology
9 for atmospheric corrosion studies, Journal of The Electrochemical Society, 14 (2011) C9-C11.

10 [5] J.A. Elliot, Novel approaches to multiscale modelling in materials science, International Materials
11 Reviews, 56 (2011) 207-225.

12 [6] I.S. Cole, N.S. Azmat, A. Kanta, M. Venkatraman, What really controls the atmospheric corrosion
13 of zinc? Effect of marine aerosols on atmospheric corrosion of zinc, International Materials Reviews,
14 54 (2009) 117-133.

15 [7] V. Maurice, P. Marcus, Passive films at the nanoscale, Electrochimica Acta, 84 (2012) 129-138.

16 [8] A.A. Franco, M. Gerard, Multiscale model of carbon corrosion in a PEFC: coupling with
17 electrocatalysis and impact on performance degradation, Journal of The Electrochemical Society,
18 155 (2008) B367-B384.

19 [9] G.D. Ingram, I.T. Cameron, K.M. Hangos, Classification and analysis of integrating frameworks in
20 multiscale modelling, Chemical Engineering Science, 59 (2004) 2171-2187.

21 [10] H. Rafii-Tabar, A. Chirazi, Multi-scale computational modelling of solidification phenomena,
22 Physics Reports, 365 (2002) 145-249.

23 [11] C.-J. Yu, Atomistic simulations for material processes within multiscale method, in: Von der
24 Fakultat fur Georessourcen und Materialtechnik Rheinisc-Westfalischen Technischen Hochschule
25 Aachen, Aachen, 2009.

26 [12] H. Tan, Combined atomistic and continuum simulation of fracture and corrosion, in:
27 Comprehensive Structural Integrity: Interfacial and Nanoscale Failure, Elsevier, Amsterdam, 2003.

- 1 [13] G.S. Frankel, M. Stratmann, Meeting report: future perspectives of corrosion science, Corrosion
2 Engineering, Science and Technology, 44 (2009) 328-331.
- 3 [14] D.A. Shifler, Factors that influence corrosion of materials and how modeling may predict these
4 effects, in: 2005 Tri-Service Corrosion Conference, NACE, Orlando FL, 2005.
- 5 [15] A. Anderko, Modeling of aqueous corrosion, in: T. Richardson, R.A. Cottis, J.D. Scantlebury, S.B.
6 Lyon, P. Skeldon, G.E. Thompson, R. Lindsay, M. Graham (Eds.) Shreir's Corrosion, ChemTec
7 Publishing Inc., Toronto, 2010, pp. 1585-1629.
- 8 [16] D. Cubicciotti, Potential-pH diagrams for alloy-water systems under LWR conditions, Journal of
9 Nuclear Materials, 201 (1993) 176-183.
- 10 [17] A. Bouzoubaa, D. Costa, B. Diawara, N. Audiffern, P. Marcus, Insight of DFT and atomistic
11 thermodynamics on the adsorption and insertion of halides onto the hydroxylated NiO(111) surface,
12 Corrosion Science, 52 (2010) 2643-2652.
- 13 [18] A. Bouzoubaa, B. Diawara, V. Maurice, C. Minot, P. Marcus, Ab initio modeling of localized
14 corrosion: study of the role of surface steps in the interaction of chlorides with passivated nickel
15 surfaces, Corrosion Science, 51 (2009) 2174-2182.
- 16 [19] A. Chakraborty, D.G. Truhlar, Quantum mechanical reaction rate constants by vibrational
17 configuration interaction: The $\text{OH} + \text{H}_2 \rightarrow \text{H}_2\text{O} + \text{H}$ reaction as a function of temperature, PNAS, 102
18 (2005) 6744-6749.
- 19 [20] D. Costa, K. Sharkas, M.M. Islam, P. Marcus, A realistic ab initio model of the passive film formed
20 on stainless steels, in: Report on Workshop Computer Simulation of Oxides: Dopants, Defects and
21 Surfaces, Trinity College, Dublin, 2009, pp. 24-25.
- 22 [21] S.C. Hendy, N.J. Laycock, M.P. Ryan, Atomistic modeling of cation transport in the passive film
23 on iron and implications for models of growth kinetics, Journal of Electrochemical Society, 152
24 (2005) B271-B276.
- 25 [22] A.S. Agarwal, U. Landau, J.H. Payer, Modeling the current distribution in thin electrolyte films
26 with applications to crevice corrosion, Journal of Electrochemical Society, 157 (2010) C9-C17.
- 27 [23] I.S. Cole, D.A. Paterson, Corrosion Engineering, Science and Technology, 39 (2004) 125-130.
- 28 [24] R.A. Cottis, Introduction to the modeling of corrosion, in: T. Richardson, R.A. Cottis, J.D.
29 Scantlebury, S.B. Lyon, P. Skeldon, G.E. Thompson, R. Lindsay, M. Graham (Eds.) Shreir's Corrosion,
30 ChemTec Publishing Inc., Toronto, 2010, pp. 1581-1584.

- 1 [25] N.J. Laycock, M.H. Moayed, J.S. Newman, Metastable pitting and the critical pitting
2 temperature, *Journal of Electrochemical Society*, 145 (1998) 2622-2628.
- 3 [26] D.D. Macdonald, The point defect model for the passive state, *Journal of Electrochemical*
4 *Society*, 139 (1992) 3434-3449.
- 5 [27] F. Mansfeld, K.B. Oldham, A modification of the Stern-Geary linear polarization equation,
6 *Corrosion Science*, 11 (1971) 787-796.
- 7 [28] P. Marcus, V. Maurice, H.-H. Strehblow, Localized corrosion (pitting): A model of passivity
8 breakdown including the role of the oxide layer nanostructure, *Corrosion Science*, 50 (2008) 2698–
9 2704.
- 10 [29] S. Scheiner, C. Hellmich, Finite volume model for diffusion- and activation- controlled pitting
11 corrosion of stainless steel, *Computer Methods in Applied Mechanics Engineering*, 198 (2009) 2898-
12 2910.
- 13 [30] S.M. Sharland, C.P. Jackson, A.J. Diver, A finite element model of the propagation of corrosion
14 crevices and pits, *Corrosion Science*, 29 (1989) 1149-1166.
- 15 [31] C. Vautrin-UI, A. Taleb, J. Stafiej, A. Chausse, J.P. Badiali, Reprint of "Mesoscopic modelling of
16 corrosion phenomena: coupling between electrochemical and meachanical processes, anlysis of the
17 deviation from the Faraday law, *Electrochimica Acta*, 52 (2007) 7802-7810.
- 18 [32] R. Reigada, F. Sagues, J.M. Costa, A Monte carlo simulation of localized corrosion, *Journal of*
19 *Chemical Physics*, 101 (1994) 2329-2337.
- 20 [33] J.L. Alamilla, E. Sosa, Stochastic modelling of corrosion damage propagation in active sites from
21 field inspection data, *Corrosion Science*, 50 (2008) 1811-1819.
- 22 [34] B. Baroux, The kinetics of pit generation on stainless steels, *Corrosion Science*, 28 (1988) 969-
23 986.
- 24 [35] A. Valor, F. Caleyó, L. Alfonso, D. Rivas, J.M. Hallen, Stochastic modeling of pitting corrosion: A
25 new model for initiation and growth of multiple corrosion pits, *Corrosion Science*, 49 (2007) 559-
26 579.
- 27 [36] D.E. Williams, C. Westcott, M. Fleischmann, Stochastic models of pitting corrosion of stainless
28 steels, *Journal of The Electrochemical Society*, 132 (1985) 1804-1811.
- 29 [37] B. Wu, J.R. Scully, J.L. Hudson, Cooperative stochastic behavior in localized corrosion, *Journal of*
30 *Electrochemical Society*, 144 (1997) 1614-1619.

- 1 [38] C. Gabrielli , F. Huet, M. Keddam, R. Oltra, A review of the probabilistic aspects of localized
2 corrosion, *Corrosion*, 46 (1990).
- 3 [39] J.V. Tu, *Journal of Clinical Epidemiology*, 49 (1996) 1225-1231.
- 4 [40] R.A. Bailey, R.M. Pidarparti, S. Jayanti, M.J. Palakal, Corrosion Prediction in Aging Aircraft
5 Materials using Neural Networks, in: 41st AIAA/ASME/ASCE/AHS/ASC Structures, Structural
6 Dynamics and Materials Conference, Atlanta, Georgia, 2000.
- 7 [41] M.K. Cavanaugh, R.G. Buchheit, N. Birbilis, Modeling the environmental dependence of pit
8 growth using neural network approaches, *Corrosion Science*, 52 (2010) 3070-3077.
- 9 [42] D. Colorado-Garrido, D.M. Ortega-Toledo, J.A. Hernández, J.G. González-Rodríguez, J.
10 Uruchurtu, Neural networks for Nyquist plots prediction during corrosion inhibition of a pipeline
11 steel

12 *Journal of Solid State Electrochemistry*, 13 (2009) 1715-1722.
- 13 [43] R.M. Pidarparti, Structural corrosion health assessment using computational intelligence
14 models, *Structural Health Monitoring*, 6 (2007) 245-259.
- 15 [44] D.V. Svintradze, R.M. Pidarparti, A theoretical model for metal corrosion degradation,
16 *International Journal of Corrosion*, 2010 (2010) 1-7.
- 17 [45] R.A. Cottis, Neural Network Methods for Corrosion Data Reduction, in: T. Richardson, R.A.
18 Cottis, J.D. Scantlebury, S.B. Lyon, P. Skeldon, G.E. Thompson, R. Lindsay, M. Graham (Eds.) Shreir's
19 Corrosion, ChemTec Publishing Inc., Toronto, 2010, pp. 1680-1692.
- 20 [46] M.H. Engelhard, D.D. Macdonald, Unification of the deterministic and statistical approaches for
21 predicting localized corrosion damage. I. Theoretical foundation, *Corrosion Science*, 46 (2004) 2755-
22 2780.
- 23 [47] N.J. Laycock, J.S. Noh, S.P. White, D.P. Krouse, Computer simulation of pitting potential
24 measurements, *Corrosion Science*, 47 (2005) 3140-3177.
- 25 [48] A. Turnbull, L.N. McCartney, S. Zhou, A model to predict the evolution of pitting corrosion and
26 the pit-to-crack transition incorporating statistically distributed input parameters, *Corrosion Science*,
27 48 (2006) 2084-2105.
- 28 [49] T. Suter, E.G. Webb, H. Bohni, R.C. Alkire, Pit initiation on stainless steels in 1M NaCl with and
29 without mechanical stress, *Journal of The Electrochemical Society*, 148 (2001) B174-B185.

- 1 [50] N. Birbilis, R.G. Buchheit, Investigation and discussion of characteristics for intermetallic phases
2 common to aluminum alloys as a function of solution pH, *Journal of The Electrochemical Society*, 155
3 (2008) C117-C126.
- 4 [51] G.D. Ingram, I.T. Cameron, Formulation and comparison of alternative multiscale models for
5 drum granulation, *Computer Aided Chemical Engineering*, 20 (2005) 481-486.
- 6 [52] C.L. Rountree, R.K. Kalia, E. Lidorikis, A. Nakano, L. Van Brutzel, P. Vashishta, Atomistic aspects
7 of crack propagation in brittle materials: Multimillion atom molecular dynamics simulations, *Annu.*
8 *Rev. Mater. Res.*, 32 (2002) 377-400.
- 9 [53] Y. Chen, J.D. Lee, A. Eskandarian, *Meshless Methods in Solid Mechanics*, Springer, 2006.
- 10 [54] N.P. Daphalapurkar, H. Lu, D. Coker, R. Komanduri, Simulation of dynamic crack growth using
11 the generalized interpolation material point (GIMP) method, *International Journal of Fracture*, 143
12 (2007) 79-102.
- 13 [55] R. Das, P.W. Cleary, Effect of rock shapes on brittle fracture using Smoothed Particle
14 Hydrodynamics, *Theoretical and Applied Fracture Mechanics*, 23 (2010) 47-60.
- 15 [56] G.R. Liu, M.B. Liu, *Smoothed particle hydrodynamics: a mesh-free particle method*, World
16 Scientific Publishing Co. Pte. Ltd., Singapore, 2003.
- 17 [57] G.S. Frankel, Pitting Corrosion, in: S.D. Cramer, J. Covino, B. S. (Eds.) *Metals handbook*, ASM
18 International, Materials Park OH, 2003.
- 19 [58] P. Marcus, *Corrosion mechanisms in theory and practice*, in, CRC Press, Boca Raton, FL, 2012.
- 20 [59] P.R. Roberge, *Handbook of Corrosion Engineering*, McGraw-Hill, New York, 2000.
- 21 [60] Z. Szklarska-Smialowska, *Pitting corrosion of metals*, NACE, 1986.
- 22 [61] X.G. Zhang, *Corrosion and Electrochemistry of Zinc*, Plenum Press, New York, 1996.
- 23 [62] S.M. Sharland, A review of the theoretical modelling of crevice and pitting corrosion, *Corrosion*
24 *Science*, 27 (1987) 289-325.
- 25 [63] G.F. Kennell, R.W. Evitts, K.L. Heppner, A critical crevice solution and IR drop crevice corrosion
26 model, *Corrosion Science*, 50 (2008) 1716-1725.

- 1 [64] M.S. Venkatraman, I.S. Cole, D.R. Gunasegaram, B. Emmanuel, Modelling corrosion of a metal
2 under an aerosol droplet, *Materials Science Forum*, 654-656 (2010) 1650-1653.
- 3 [65] N.C. Barnard, S.G.R. Brown, Modelling the relationship between microstructure of Galfan-type
4 coated steel and cut-edge corrosion resistance incorporating diffusion of multiple species, *Corrosion*
5 *Science*, 50 (2008) 2846-2857.
- 6 [66] S.G.R. Brown, N.C. Barnard, 3D computer simulation of the influence of microstructure on the
7 cut edge corrosion behaviour of a zinc aluminium alloy galvanized steel, *Corrosion Science*, 48 (2006)
8 2291-2303.
- 9 [67] M.A. Jakob, D.A. Little, J.R. Scully, Experimental and modelling studies of the oxygen reduction
10 reaction on AA2024-T3., *Journal of Electrochemical Society*, 152 (2005) B311-B320.
- 11 [68] W. Zhang, S. Ruan, D.A. Wolfe, F. G.S., Statistical model for intergranular corrosion growth
12 kinetics, *Corrosion Science*, 45 (2003) 353-370.
- 13 [69] M.K. Cavanaugh, R.G. Buchheit, N. Birbilis, Evaluation of a simple microstructural-
14 electrochemical model for corrosion damage accumulation in microstructurally complex aluminum
15 alloys, *Engineering Fracture Mechanics*, 76 (2009) 641-650.
- 16 [70] X. Zhou, C. Luo, T. Hashimoto, A.E. Hughes, G.E. Thompson, Study of localized corrosion in
17 AA2024 aluminium alloy using electron tomography, *Corrosion Science*, 58 (2012) 299-306.
- 18 [71] M. Rappaz, C.A. Gandin, Probabilistic modeling of microstructure formation in solidification
19 processes, *Acta Metallurgica Materialia*, 41 (1993) 345-360.
- 20 [72] S. Hao, W.K. Liu, B. Moran, F.J. Vernery, G.B. Olson, Multi-scale constitutive model and
21 computational framework for the design of ultra-high strength, high toughness steels, *Computer*
22 *Methods in Applied Mechanics Engineering*, 193 (2004) 1865-1908.
- 23 [73] F.J. Vernery, W.K. Liu, B. Moran, G. Olson, A micromorphic model for the multiple scale failure
24 of heterogeneous materials, *Journal of the Mechanics and Physics of Solids*, 56 (2008) 1320-1347.
- 25 [74] P.D. Lee, A. Chirazi, R.C. Atwood, W. Wang, Multiscale modelling of solidification
26 microstructures, including microsegregation and microporosity, in an Al-Si-Cu alloy, *Materials*
27 *Science and Engineering A*, 365 (2004) 57-65.
- 28 [75] J. Wang, M. Li, J. Allison, P.D. Lee, Multiscale modeling of the influence of Fe content in a Al-Si-
29 Cu alloy on the size distribution of intermetallic phases and micropores, *Journal of Applied Physics*,
30 107 (2010).

- 1 [76] J.S. Wang, P.D. Lee, Simulating tortuous 3D morphology of microporosity formed during the
2 solidification of Al-Si-Cu alloys, *International Journal of Cast Metals Research*, 20 (2007) 151-158.
- 3 [77] L. Tan, K. Sridharan, T.R. Allen, Altering corrosion response via grain boundary engineering,
4 *Materials Science Forum*, 595-598 (2008) 409-418.
- 5 [78] D. Bombac, Atomistic simulations of precipitation kinetics in multicomponent
6 interstitia/substitutional alloys, in: Department of Materials and Metallurgy, University of Ljubljana,
7 Ljubljana, 2012.
- 8 [79] D. Kempf, V. Vignal, N. Martin, S. Virtanen, Relationships between strain, microstructures and
9 oxide growth at the nano- and microscale, *Surface and Interface Analysis*, 40 (2008) 43-50.
- 10 [80] Y. Osada, Electron probe microanalysis (EPMA) measurement of aluminum oxide film thickness
11 in the nanometer range on aluminum sheets, *X-Ray Spectrometry*, 34 (2005) 92-95.
- 12 [81] J.K. Thomas, R.S. Ondrejcin, Aluminum oxide film thickness and emittance (U), in: Report No.
13 WSRC-RD-91-24 TASK 91-080-1, Savannah River Laboratory, Aiken SC 29808, 1991.
- 14 [82] T.E. Graedel, Corrosion Mechanisms for Zinc Exposed to the Atmosphere, *Journal of*
15 *Electrochemical Society*, 136 (1989) 193C-203C.
- 16 [83] H.-H. Strehblow, Passivity of metals, in: R.C. Alkire, D.M. Kolb (Eds.) *Advances in Electrochemical*
17 *Science and Engineering* Wiley-VCH, Weinheim, 2003, pp. 271-374.
- 18 [84] L.P.H. Jeurgens, W.G. Sloof, F.D. Tichelaar, E.J. Mittemeijer, Thermodynamic stability of
19 amorphous oxide films on metals: application to aluminum oxide films on aluminum substrates,
20 *Physicsl Review B*, 62 (2000) 4707-4719.
- 21 [85] I.S. Cole, T.H. Muster, S.A. Furman, N. Wright, A. Bradbury, Products Formed during the
22 Interaction of Seawater Droplets with Zinc Surfaces: I. Results from 1- and 2.5-Day Exposures,
23 *Journal of Electrochemical Society*, 155 (2008) C244-C255.
- 24 [86] D. Lau, A.M. Glenn, A.E. Hughes, F.H. Scholes, T.H. Muster, S.G. Hardin, Factors influencing the
25 deposition of Ce-based conversion coatings, Part II: The role of localised reactions, *Surface and*
26 *Coatings Technology*, 203 (2009) 2937-2945.
- 27 [87] L. Sziraki, I. Cziraki, Z. Vertesy, L. Kiss, A kinetic model of the spontaneous passivation and
28 corrosion of zinc in near neutral Na₂SO₄ solutions, *Electrochimica Acta*, 43 (1998) 175-186.
- 29 [88] Z. Szklarska-Smialowska, Pitting corrosion of aluminum, *Corrosion Science*, 41 (1999) 1743-
30 1767.

- 1 [89] A.E. Hughes, F.H. Scholes, A.M. Glenn, D. Lau, T.H. Muster, S.G. Hardin, Factors influencing the
2 deposition of Ce-based conversion coatings, part I: The role of Al³⁺ ions, *Surface & Coatings*
3 *Technology*, 203 (2009) 2927-2936.
- 4 [90] P.A. White et al, High-throughput channel arrays for inhibitor testing: Proof of concept for
5 AA2024-T3, *Corrosion Science*, 51 (2009).
- 6 [91] D.D. Macdonald, Kinetic Stability Diagrams, in: *ECS Transactions, The Electrochemical Society,*
7 *Cancun, Mexico, 2007*, pp. 403-418.
- 8 [92] X. Zhou, N. Birbilis, D.D. Macdonald, Kinetic stability of aluminium, in: *Proceedings of the*
9 *Conference on Corrosion and Prevention '10, ACA, Adelaide, Australia, 2010*, pp. Paper 102.
- 10 [93] M.-H. Wang, K.R. Hebert, Metal and oxygen ion transport during ionic conduction in amorphous
11 anodic oxide films, *Journal of Electrochemical Society*, 146 (1999) 3741-3749.
- 12 [94] E.R. Vago, E.J. Calvo, M. Stratmann, Electrocatalysis of oxygen reduction at well-defined iron
13 oxide electrodes, *Electrochimica Acta*, 39 (1994) 1655-1659.
- 14 [95] Z.Y. Chen, F. Cui, R.G. Kelly, Calculations of the cathodic current delivery capacity and stability of
15 crevice corrosion under atmospheric environments, *Journal of Electrochemical Society*, 155 (2008)
16 C360-C368.
- 17 [96] F. Mansfeld, J.V. Kenkel, Laboratory studies of galvanic corrosion: I. Two-metal couples,
18 *Corrosion*, 31 (1975) 298-302.
- 19 [97] M.S. Venkatraman, I.S. Cole, B. Emmanuel, Corrosion under a porous layer: a porous electrode
20 model and its implications for self-repair, *Electrochimica Acta*, 56 (2011) 8192-8203.
- 21 [98] D. Rodney, T. A., V. D., Modeling the mechanics of amorphous solids at different length scale
22 and time scale, *Model Simul Mater Sc*, 19 (2011) 083001.
- 23 [99] D.E. Williams, M.R. Kilburn, J. Cliff, G.I.N. Waterhouse, Composition changes around sulphide
24 inclusions in stainless steels, and implications for the initiation of pitting corrosion, *Corrosion*
25 *Science*, 52 (2010) 3702-3716.
- 26 [100] D.-H. Kim, G.-W. Lee, Y.-C. Kim, Interaction of zinc interstitial with oxygen vacancy in zinc oxide:
27 an origin of n-type doping, *Solid State Communications*, 152 (2012) 1711-1714.
- 28 [101] B. Diawara, Y.-A. Beh, P. Marcus, Atomistic simulation of the passivation of iron-chromium
29 alloys using calculated local diffusion activation barriers, in: P. Marcus (Ed.) *Passivation of Metals*
30 *and Semiconductors and Properties of Thin Oxide*, Elsevier, 2006.

- 1 [102] F.U. Renner, A. Stierle, H. Dosch, D.M. Kolb, T.-L. Lee, J. Zegenhagen, Initial corrosion observed
2 on the atomic scale, *Nature*, 439 (2006) 707-710.
- 3 [103] A. Seyeux, V. Maurice, L.H. Klein, P. Marcus, Initiation of localized corrosion at the nanoscale
4 by competitive dissolution and passivation of nickel surfaces, *Electrochimica Acta*, 54 (2008) 540-
5 544.
- 6 [104] D.D. Macdonald, Passivity- the key to our metal-based civilization, *Pure and Applied Chemistry*,
7 71 (1999) 951-978.
- 8 [105] K.R. Zavadil, J.A. Ohlhausen, P.G. Kotula, Nanoscale void nucleation and growth in the passive
9 oxide on aluminum as a pre-pitting process, *Journal of The Electrochemical Society*, 153 (2006) B296-
10 B303.
- 11 [106] Anon., A DETERMINISTIC MODEL FOR CORROSION AND ACTIVITY INCORPORATION IN
12 NUCLEAR POWER PLANTS, in:
13 www.vtt.fi/liitetiedostot/muut/ANTIOXI%20AB%20060207%20VTT.ppt, VTT Technical Research
14 Center of Finland, 2007.
- 15 [107] H. Ding, L.H. Hihara, Corrosion initiation and anodic-cathodic alteration of localized corrosion
16 of SiC-reinforced aluminum matrix composites in NaCl solution, *ECS Transactions*, 3 (2007) 237-247.
- 17 [108] J. Toth, Adsorption Theory, Modeling and Analysis, in, Marcel Dekker, New York, 2002.
- 18 [109] A. Anderko, N. Sridhar, L.T. Yang, S.L. Grise, B.J. Saldanha, M.H. Dorsey, Validation of localised
19 corrosion model using real time corrosion monitoring in a chemical plant, *Corrosion Engineering
20 Science and Technology*, 40 (2005) 33-42.
- 21 [110] L.A. Farrow, T.E. Graedel, C. Leygraf, GILDES model studies of aqueous chemistry. II. The
22 corrosion of zinc in gaseous exposure chamber, *Corrosion Science*, 38 (1996) 2181.
- 23 [111] U.F. Franck, R. FitzHugh, Periodische Electrodenprozesse und ihre Beschreibung durch
24 Mathematische Modell, *Zeitschrift fuer Electrochemie* 65 (1961) 156.
- 25 [112] T.P. Hoar, W.R. Jacob, Breakdown of passivity of stainless steel by halide ions, *Nature*, 216
26 (1967) 1299-1301.
- 27 [113] E. McCafferty, Sequence of steps in the pitting of aluminum by chloride ions, *Corrosion
28 Science*, 45 (2003) 1421-1438.
- 29 [114] T. Okada, Considerations of the stability of pit repassivation during pitting corrosion of passive
30 metals, *Journal of the Electrochemical Society*, 131 (1984) 1026-1032.

- 1 [115] G.S. Frankel, N. Sridhar, Understanding localized corrosion, in: Materials Today, Elsevier, 2008,
2 pp. 38-44.
- 3 [116] D.D. Macdonald, On the existence of our metals-based civilization I. Phase-Space Analysis,
4 Journal of The Electrochemical Society, 153 (2006) B213.
- 5 [117] B. Krishnamurthy, R.E. White, H.J. Ploehn, Simplified point defect model for growth of anodic
6 passive films on iron, Electrochimica Acta, 47 (2002) 3375-3381.
- 7 [118] G. Gece, The use of quantum chemical methods in corrosion inhibitor studies, Corros Sci, 50
8 (2008) 2981-2992.
- 9 [119] G. Gece, S. Bilgic, Molecular-Level Understanding of the Inhibition Efficiency of Some Inhibitors
10 of Zinc Corrosion by Quantum Chemical Approach, Ind. Eng. Chem. Res., 51 (2012) 14115-14120.
- 11 [120] D.S. Sholl, J.A. Steckel, Density Functional Theory: A Practical Introduction, John Wiley & Sons
12 Inc, Hoboken NJ, 2009.
- 13 [121] C.D. Taylor, Atomistic modeling of corrosion events at the interface between a metal and its
14 environment, International Journal of Corrosion, 2012 (2012) 1-13.
- 15 [122] G. Gece, The use of quantum chemical methods in corrosion inhibitor studies, Corrosion
16 Science, 50 (2008) 2981-2992.
- 17 [123] C.M. Goulart et al, Experimental and theoretical evaluation of semicarbazones and
18 thiosemicarbazones as organic corrosion inhibitors, Corrosion Science, 67 (2013) 281-291.
- 19 [124] M.I. Janik, C.D. Taylor, M. Neurock, First-Principles Analysis of the Initial Electroreduction Steps
20 of Oxygen over Pt(111), Journal of Electrochemical Society, 156 (2009) B126-B135.
- 21 [125] K.F. Khaled, Studies of iron corrosion inhibition using chemical, electrochemical and computer
22 simulation techniques, Electrochimica Acta, 55 (2010) 6523-6532.
- 23 [126] A. Kokalj, S. Peljhan, M. Finsgar, I. Milosev, What determines the inhibition effectiveness of
24 ATA, BTAH and BTAOH corrosion inhibitors on copper?, Journal of the American Chemical Society,
25 132 (2010) 16657-16668.
- 26 [127] A.Y. Musa, Corrosion Inhibition of Mild Steel in 1.0 M HCl by Amino Compound:
27 Electrochemical and DFT Studies, Metallurgical and Materials Transactions A, 43A (2012) 3379-3386.

- 1 [128] J.M. Soler, E. Artacho, J.D. Gale, A. Garcia, J. Junquera, P. Ordejon, D. Sanchez-Portal, The
2 SIESTA method for ab initio order-N materials simulation, *Journal of Physics: Condensed Matter*, 14
3 (2002) 2745-2779.
- 4 [129] K.Y. Yeh, Density Functional Theory-Based Electrochemical Models for the Oxygen Reduction
5 Reaction: Comparison of Modeling Approaches for Electric Field and Solvent Effects, *Journal of*
6 *Computational Chemistry*, 32 (2011) 3399-3408.
- 7 [130] L.C. Abodi, et al., , *Modeling localized aluminum alloy corrosion in chloride solutions under non-*
8 *equilibrium conditions: Steps toward understanding pitting initiation*, *Electrochimica Acta*, 63 (2012)
9 169-178.
- 10 [131] T.G. Harvey, et al, *The effect of inhibitor structure on the corrosion of AA2024 and AA7075*,
11 *Corrosion Science*, 53 (2011) 2184-2190.
- 12 [132] T. Arslan, et al., *Quantum chemical studies on the corrosion inhibition of some sulphonamides*
13 *on mild steel in acidic medium*, *Corrosion Science*, 51 (2009) 35-47.
- 14 [133] K.F. Khaled, N.S. Abdel-Shafi, *Quantitative Structure and Activity Relationship Modeling Study*
15 *of Corrosion Inhibitors: Genetic Function Approximation and Molecular Dynamics Simulation*
16 *Methods*, *International Journal of Electrochemical Science*, 6 (2011) 4077-4094.
- 17 [134] A.Y. Musa, et al., *Quantum chemical studies on corrosion inhibition for series of thio*
18 *compounds on mild steel in hydrochloric acid*, *Journal of Industrial and Engineering Chemistry*, 18
19 (2012) 551-555.
- 20 [135] Z. El Adnani, et al., . , 2013. **68**: p. 223-230., *DFT theoretical study of 7-R-3methylquinoxalin-*
21 *2(1H)-thiones (R=H; CH₃; Cl) as corrosion inhibitors in hydrochloric acid*, *Corrosion Science*, 68 (2013)
22 223-230.
- 23 [136] A. Kokalj, . , 2013. **68**: p. 195-203., *Formation and structure of inhibitive molecular film of*
24 *imidazole on iron surface*, *Corrosion Science*, 68 (2013).
- 25 [137] M. Dion, *Van der Waals density functional for general geometries*, *Physical Review Letters*, 92
26 (2004).
- 27 [138] O.A. von Lilienfeld, *Optimization of effective atom centered potentials for London dispersion*
28 *forces in density functional theory*, *Physical Review Letters*, 93 (2004).
- 29 [139] Y. Zhao, D.G. Truhlar, *The M06 suite of density functionals for main group thermochemistry,*
30 *thermochemical kinetics, noncovalent interactions, excited states, and transition elements: two new*
31 *functionals and systematic testing of four M06-class functionals and 12 other functionals*, *Theoretical*
32 *Chemistry Accounts*, 120 (1-3) (2008) 215-241.

- 1 [140] S. Grimme, *Semiempirical GGA-type density functional constructed with a long-range*
2 *dispersion correction.*, *Journal of Computational Chemistry*, 27 (2006) 1787-1799.
- 3 [141] E. Spohr, Some recent trends in the computer simulations of aqueous double layers,
4 *Electrochimica Acta*, 49 (2003) 23-27.
- 5 [142] D.T. Taylor, R.G. Kelly, M. Neurock, First-principles prediction of equilibrium potentials for
6 water activation by a series of metals, *Journal of The Electrochemical Society*, 154 (2007) F217-F221.
- 7 [143] K.Y. Yeh, M.J. Janik, Density Functional Theory-Based Electrochemical Models for the Oxygen
8 Reduction Reaction: Comparison of Modeling Approaches for Electric Field and Solvent Effects, *J.*
9 *Comput. Chem.*, 32 (2011) 3399-3408.
- 10 [144] C.D. Taylor, S.A. Wasileski, J.S. Filhol, M. Neurock, First principles reaction modeling of the
11 electrochemical interface: Consideration and calculation of a tunable surface potential from atomic
12 and electronic structure, *Phys. Rev. B*, 73 (2006).
- 13 [145] S. Fletcher, The theory of electron transfer, *Journal of Solid State Electrochemistry*, 14 (2010)
14 705-739.
- 15 [146] M.V. Sangaranarayanan, K.L. Sebastian, *Theoretical Chemistry and Electrochemistry*, *Journal of*
16 *Chemical Sciences*, 121 (2009) 559-560.
- 17 [147] A. Winkler, J. Horbach, W. Kob, K. Binder, Structure and diffusion in amorphous aluminum
18 silicate: A molecular dynamics computer simulation, *Journal of Chemical Physics*, 120 (2004) 384-
19 393.
- 20 [148] M.M. Islam, B. Diawara, V. Maurice, P. Marcus, Atomistic modeling of voiding mechanisms at
21 oxide/alloy Interfaces, *The Journal of Physical Chemistry*, 113 (2009) 9978-9981.
- 22 [149] K.F. Khaled, Studies of iron corrosion inhibition using chemical, electrochemical and computer
23 simulation techniques, *Electrochimica Acta*, 55 (2010) 6523-6532.
- 24 [150] R. Baboian, *Corrosion tests and standards: application and interpretation*, ASTM International,
25 Philadelphia PA, 2005.
- 26 [151] J.L. Kennedy, *Oil and gas pipeline fundamentals*, 2nd ed., PennWell Publishing Company, Tulsa
27 OK, 1993.
- 28 [152] C. Arya, P.R.W. Vassie, Influence of cathode-to-anode area ratio and separation distance on
29 galvanic corrosion currents of steel in concrete containing chlorides, *Cement and Concrete Research*,
30 25 (1995) 989-998.

- 1 [153] N. Birbilis, R.G. Buchheit, Electrochemical characteristics of intermetallic phases in aluminum
2 alloys - An experimental survey and discussion, *Journal of The Electrochemical Society*, 152 (2005)
3 B140-B151.
- 4 [154] M.G. Fontana, *Corrosion Engineering*, 3rd ed., Mc-Graw Hill Book Company, New York, 1986.
- 5 [155] L.F. Garfias-Mesias, J.M. Sykes, The Influence of Cu on the Pitting Corrosion of Duplex Stainless
6 Steel UNS S32550, in: *CORROSION 96*, Denver, Co, 1996.
- 7 [156] D.A. Jones, *Principles and Prevention of Corrosion*, 2nd ed., Prentice-Hall, Upper Saddle River
8 NJ, 1996.
- 9 [157] W.W. Kirk, *Atmospheric corrosion*, American Society for Testing Materials, Materials Park OH,
10 1995.
- 11 [158] L. Lacroix, L. Ressler, C. Blanc, G. Mankowskia, Combination of AFM, SKPFM, and SIMS to Study
12 the Corrosion Behavior of S-phase particles in AA2024-T351, *Journal of Electrochemical Society*, 155
13 (2008) C131-C137.
- 14 [159] J. Koleske, V., *Paint and coating testing manual: fourteenth edition of the Gardner-Sward*
15 *handbook*, ASTM, Philadelphia PA, 1995.
- 16 [160] R. Alkire, D. Siitari, The location of cathodic reaction during localized corrosion, *Journal of The*
17 *Electrochemical Society*, 126 (1979) 15-22.
- 18 [161] M.A. Alodan, Modeling of pH distribution over corrosion sites, *Journal of the King Saud*
19 *University*, 15 (2002) 1-12.
- 20 [162] C. Vautrin-UI, H. Mendy, A. Taleb, A. Chausse, J. Stafiej, J.P. Badiali, Numerical simulations of
21 heterogeneity formation in metal corrosion, *Corrosion Science*, 50 (2008) 2149-2158.
- 22 [163] O.M. Magnussen, L. Zitzler, B. Gleich, M.R. Vogt, R.J. Behm, In-situ atomic-scale studies of the
23 mechanisms and dynamics of metal dissolution by high-speed STM, *Electrochimica Acta*, 46 (2001)
24 3725-3733.
- 25 [164] D.E. Williams, T.F. Mohiuddin, Y.Y. Zhu, Elucidation of a Trigger Mechanism for Pitting
26 Corrosion of Stainless Steels Using Submicron Resolution Scanning Electrochemical and
27 Photoelectrochemical Microscopy, *Journal of The Electrochemical Society*, 145 (1998) 2664-2672.
- 28 [165] E.M. Sevick, R. Prabhakar, S.R. Williams, D.J. Searles, Fluctuation theorems, *Annual Review of*
29 *Physical Chemistry*, 59 (2008) 603-633.

- 1 [166] M. Legrand, B. Diawara, J.-J. Legendre, P. Marcus, Three-dimensional modelling of selective
2 dissolution and passivation of iron-chromium alloys, *Corrosion Science*, 44 (2002) 773-790.
- 3 [167] D.E. Williams, J. Stewart, P.H. Balkwill, The nucleation, growth and stability of micropits in
4 stainless steel, *Corrosion Science*, 36 (1994) 1213-1235.
- 5 [168] H. Wang, J. Xie, K.P. Yan, M. Duan, Y. Zuo, The nucleation and growth of metastable pitting on
6 pure iron, *Corrosion Science*, 51 (2009) 181-185.
- 7 [169] N. Budiansky, L. Organ, A.S. Mikhailov, J.L. Hudson, J.R. Scully, Co-operative spreading of pit
8 sites as a new explanation for critical threshold potentials, in: P. Schmuki (Ed.) *Pits and Pores III:
9 Formation, Properties, and Significance for Advanced Materials*, The Electrochemical Society, 2004,
10 pp. 313-324.
- 11 [170] A.S. Mikhailov, J.R. Scully, J.L. Hudson, Nonequilibrium collective phenomena in the onset of
12 pitting corrosion, *Surface Science*, 603 (2009) 1912-1921.
- 13 [171] J.R. Scully, N.D. Budiansky, Y. Tiwary, A.S. Mikhailov, J.L. Hudson, An alternate explanation for
14 the abrupt current increase at the pitting potential, *Corrosion Science*, 50 (2008) 316-324.
- 15 [172] G.S. Frankel, Pitting corrosion of metals: a review of the critical factors, *Journal of*
16 *Electrochemical Society*, 145 (1998) 2186-2198.
- 17 [173] G.T. Burstein, P.C. Pistorius, S.P. Mattin, The nucleation and growth of corrosion pits on
18 stainless steel, *Corrosion Science*, 35 (1993) 57-62.
- 19 [174] H. Ezuher, R.C. Newman, Growth-Rate Distribution of Metastable Pits, in: G.S. Frankel, R.C.
20 Newman (Eds.) *Critical factors in Localized Corrosion*, The Electrochemical Society, Pennington NJ,
21 1992, pp. 120.
- 22 [175] M.A. Baker, J.E. Castle, The initiation of pitting corrosion at MnS inclusions, *Corrosion Science*,
23 34 (1993) 667-682.
- 24 [176] R. Ke, R. Alkire, Surface analysis of corrosion pits initiated at MnS inclusions in 304 stainless
25 steel, *Journal of The Electrochemical Society*, 139 (1993) 1573-1580.
- 26 [177] M.P. Ryan, D.E. Williams, R.J. Chater, B.M. Hutton, D.S. McPhall, Why stainless steel corrodes,
27 *Nature*, 415 (2002) 770-774.
- 28 [178] R.M. Rynders, C.-H. Paik, R. Ke, R.C. Alkire, Use of in situ atomic force microscopy to image
29 corrosion at inclusions, *Journal of The Electrochemical Society*, 141 (1994) 1439-1445.

- 1 [179] G. Wranglen, Pitting and sulphide inclusions in steel, *Corrosion Science*, 14 (1974) 331-349.
- 2 [180] T. Shibata, T. Takeyama, Stochastic Theory of Pitting Corrosion, *Corrosion*, 33 (1977) 243-251.
- 3 [181] C. Punckt, M. Bolscher, H.H. Rotermund, A.S. Mikhailov, L. Organ, N. Budiansky, J.R. Scully, J.L.
4 Hudson, Sudden onset of pitting corrosion on stainless steel as a critical phenomenon, *Science*, 305
5 (2004) 1133-1136.
- 6 [182] L. Organ, J.R. Scully, A.S. Mikhailov, J.L. Hudson, A spatiotemporal model of interactions among
7 metastable pits and the transition to pitting corrosion, *Electrochimica Acta*, 51 (2005) 225-241.
- 8 [183] J.C. Walton, G. Cragolino, S.K. Kalandros, A numerical model of crevice corrosion for passive
9 and active metals, *Corrosion Science*, 38 (1996) 1-18.
- 10 [184] L. Lei, L. Xiaogang, D. Chaofang, X. Kui, L. Lin, Cellular automata modeling on pitting current
11 transients, *Electrochemistry Communications*, 11 (2009) 1826-1829.
- 12 [185] B. Malki, B. Baroux, Computer simulation of the corrosion pit growth, *Corrosion Science*, 47
13 (2005) 171-182.
- 14 [186] B. Malki, B. Baroux, Study of metastable pitting of stainless steels by computer simulations, in:
15 *Proceedings of the COMSOL Users' Conference*, COMSOL inc., Paris, 2005.
- 16 [187] B. Malki, B. Baroux, Modeling of metastable pitting: towards a better understanding of the
17 effect of alloying elements in: *ECS transactions*, The Electrochemical Society, Washington DC, 2007,
18 pp. 273-284.
- 19 [188] S. Hoerle, B. Malki, B. Baroux, Corrosion Current Fluctuations at Metastable to Stable Pitting
20 Transition of Aluminum, *Journal of The Electrochemical Society*, 153 (2006) B527-B532.
- 21 [189] J.W. Cobb, *Journal of the Iron and Steel Institute*, 83 (1911) 170.
- 22 [190] K. Sasaki, H.S. Isaacs, Origins of electrochemical noise during pitting corrosion of aluminum,
23 *Journal of The Electrochemical Society*, 151 (2004) B124-B133.
- 24 [191] H.-H. Strehblow, Mechanisms of Pitting Corrosion, in: P. Marcus, J. Oudar (Eds.) *Corrosion
25 Mechanisms in Theory and Practice*, Marcel Dekker, 1995.
- 26 [192] E.G. Webb, T. Suter, R.C. Alkire, Microelectrochemical Measurements of the Dissolution of
27 Single MnS Inclusions, and the Prediction of the Critical Conditions for Pit Initiation on Stainless
28 Steel, *Journal of the Electrochemical Society*, 148 (2001) B186-B195.

- 1 [193] M. Janik-Czachor, G.C. Wood, G.E. Thompson, Assessment of the processes leading to pit
2 nucleation, *British Corrosion Journal*, 15 (1980) 153-161.
- 3 [194] J.R. Galvele, Transport processes and the mechanism of pitting in metals, *Journal of*
4 *Electrochemical Society*, 123 (1976) 464-474.
- 5 [195] J.R. Galvele, Transport processes in passivity breakdown - II: full hydrolysis of the metal ions,
6 *Corrosion Science*, 21 (1981) 551-579.
- 7 [196] S.M. Gravano, J.R. Galvele, Transport processes in passivity breakdown - III. Full hydrolysis plus
8 ion migration plus buffers, *Corrosion Science*, 24 (1984) 517-534.
- 9 [197] M.K. Sawford, B.G. Ateya, A.M. Abdullah, H.W. Pickering, The Role of Oxygen on the Stability of
10 Crevice Corrosion, *Journal of Electrochemical Society*, 149 (2002) B198-B205.
- 11 [198] N.J. Laycock, S.P. White, Computer simulation of single pit propagation in stainless steel under
12 potentiostatic control, *Journal of Electrochemical Society*, 148 (2001) B264-B275.
- 13 [199] S. Scheiner, C. Hellmich, Stable pitting corrosion of stainless steel as diffusion-controlled
14 dissolution process with a sharp moving electrode boundary, *Corrosion Science*, 49 (2007) 319-346.
- 15 [200] S. Papavinasam, R.W. Revie, W.I. Friesen, A. Doiron, T. Panneerselvam, Review of models to
16 predict internal pitting corrosion of oil and gas pipelines, *Corrosion Reviews*, 24 (2006) 173-230.
- 17 [201] R. Newman, Pitting corrosion of metals, in: *The Electrochemical Society Interface*, 2010, pp.
18 33-37.
- 19 [202] R. Alkire, D. Siitari, Initiation of crevice corrosion II. Mathematical model for aluminum in
20 sodium chloride solutions, *Journal of The Electrochemical Society*, 129 (1982) 488-496.
- 21 [203] S.M. Sharland, A mathematical model of the initiation of crevice corrosion in metals, *Corrosion*
22 *Science*, 33 (1992) 183-201.
- 23 [204] N.J. Laycock, R.C. Newman, Localised dissolution kinetics, salt films and pitting potentials,
24 *Corrosion Science*, 39 (1997) 1771-1790.
- 25 [205] H. Cong, H.T. Michels, J.R. Scully, Passivity and Pit Stability Behavior of Copper as a Function of
26 Selected Water Chemistry Variables, *Journal of The Electrochemical Society*, 156 (2009) C16-C27.
- 27 [206] D.E. Williams, R.C. Newman, Q. Song, R.G. Kelly, Passivity breakdown and pitting corrosion of
28 binary alloys, *Nature*, 350 (1991) 216-219.

- 1 [207] S. Qian, R.C. Newman, R.A. Cottis, K. Sieradzki, Computer simulation of alloy passivation and
2 activation, *Corrosion Science*, 31 (1990) 621-626.
- 3 [208] K. Sieradzki, R.C. Newman, A Percolation Model for Passivation in Stainless Steels, *Journal of*
4 *The Electrochemical Society: Accelerated Brief Communication*, (1986) 1979-1980.
- 5 [209] S.N. Rashkeev, K.W. Sohlberg, S. Zhuo, S.T. Pantelides, Hydrogen-induced initiation of
6 corrosion in aluminum, *Journal of Physical Chemistry C*, 111 (2007) 7175-7178.
- 7 [210] C.-L. Chang, S.K.R.S. Sankaranarayanan, M.H. Engelhard, V. Shutthanandan, S. Ramanathan, On
8 the Relationship between Nonstoichiometry and Passivity Breakdown in Ultrathin Oxides: Combined
9 Depth-Dependent Spectroscopy, Mott-Schottky Analysis, and molecular Dynamics Simulation
10 Studies, *Journal of Physical Chemistry C*, 113 (2009) 3502-3511.
- 11 [211] A. Seyeux, V. Maurice, P. Marcus, Breakdown kinetics at nanostructure defects of passive films,
12 *Electrochemical and Solid State Letters*, 12 (2009) C25-C27.
- 13 [212] T. Hong, M. Nagumo, Effect of surface roughness on early stages of pitting corrosion of Type
14 301 stainless steel, *Corrosion Science*, 39 (1997) 1665-1672.
- 15 [213] D.L. Olson, A. Lasseigne, N., M. Marya, B. Mishra, Weld features that differentiate weld and
16 plate corrosion, *Practical Failure Analysis*, 3 (2003) 43-57.
- 17 [214] A. Turnbull, Review of modelling of pit propagation kinetics, *British Corrosion Journal*, 28
18 (1993) 297-308.
- 19 [215] D.D. Macdonald, G.R. Engelhardt, Predictive modeling of corrosion, in: T. Richardson, R.A.
20 Cottis, J.D. Scantlebury, S.B. Lyon, P. Skeldon, G.E. Thompson, R. Lindsay, M. Graham (Eds.) *Shreir's*
21 *Corrosion*, ChemTec Publishing Inc., Toronto, 2010, pp. 1630-1679.
- 22 [216] H.W. Pickering, On the roles of corrosion products in local cell processes, *Corrosion*, 42 (1986).
- 23 [217] H.W. Pickering, R.P. Frankenthal, On the mechanism of localized corrosion of iron and stainless
24 steel; I. Electrochemical studies, *Journal of The Electrochemical Society*, 119 (1972) 1297-1304.
- 25 [218] S.M. Sharland, P.W. Tasker, A mathematical model of crevice and pitting corrosion - I. The
26 physical model, *Corrosion Science*, 28 (1988) 603-620.
- 27 [219] G. Engelhardt, M. Urquidi-Macdonald, D.D. Macdonald, A simplified method for estimating
28 corrosion cavity growth rates, *Corrosion Science*, 39 (1997) 419-441.

- 1 [220] C. Hartnig, M.T.M. Koper, Molecular dynamics simulation of the first electron transfer step in
2 the oxygen reduction reaction, *Journal of Electroanalytical Chemistry*, 532 (2002) 165-170.
- 3 [221] M.T.M. Koper, G.A. Voth, A theory for adiabatic bond breaking electron transfer reactions at
4 metal electrodes, *Chemical Physics Letters*, 282 (1998) 100-106.
- 5 [222] D.D. Macdonald, in, Email dated 24 August, 2013.
- 6 [223] Z.Y. Chen, R.G. Kelly, Computational Modeling of Bounding Conditions for Pit Size on Stainless
7 Steel in Atmospheric Environments, *Journal of The Electrochemical Society*, 157 (2010) C69-C78.
- 8 [224] H.W. Pickering, The significance of the local electrode potential within pits, crevices and cracks,
9 *Corrosion Science*, 29 (1989) 325-341.
- 10 [225] S.A.M. Refaey, Inhibition of steel pitting corrosion in HCl by some inorganic anions *Applied*
11 *Surface Science*, 240 (2005) 396-404.
- 12 [226] A. Turnbull, The solution composition and electrode potential in pits, crevices and cracks,
13 *Corrosion Science*, 23 (1983) 833-870.
- 14 [227] R.W. Evitts, Modelling of crevice corrosion, in: Department of Chemical Engineering, University
15 of Saskatchewan, Saskatchewan, 1997.
- 16 [228] S.P. White, G.J. Weir, N.J. Laycock, Calculating chemical concentrations during the initiation of
17 crevice corrosion, *Corrosion Science*, 42 (2000) 605-629.
- 18 [229] A. Alavi, R.A. Cottis, The determination of pH, potential and chloride concentration in
19 corroding crevices on 304 stainless steel and 7475 aluminium alloy, *Corrosion Science*, 27 (1987)
20 443-451.
- 21 [230] C. Taxen, D. Persson, Zinc corrosion in a crevice, in: Proceedings of the COMSOL Conference,
22 Hannover, 2008.
- 23 [231] K.L. Heppner, R.W. Evitts, J. Postlethwaite, Effect of Ionic Interactions on the Initiation of
24 Crevice Corrosion in Passive Metals, *Journal of The Electrochemical Society*, 152 (2005) B89-B98.
- 25 [232] K.S. Pitzer, Thermodynamics of electrolytes, I. Theoretical basis and general equations, *Journal*
26 *of Physical Chemistry*, 77 (1973) 268-277.
- 27 [233] A. Anderko, P. McKenzie, R.D. Young, Computation rates of general corrosion using
28 electrochemical and thermodynamic models, *Corrosion*, 57 (2001) 202-213.

- 1 [234] Activity coefficients in electrolyte solutions, in: K.S. Pitzer (Ed.), CRC Press, Boca aton FL, 1991.
- 2 [235] S. Chowdhuri, A. Chandra, Dynamics of ionic and hydrophobic solutes in water-methanol
3 mixtures of varying composition, *Journal of Chemical Physics*, 123 (2005) 234501-234509.
- 4 [236] A.P. Lyubartsev, A. Laaksonen, Concentration Effects in Aqueous NaCl Solutions. A Molecular
5 Dynamics Simulation, *Journal of Chemical Physics*, 100 (1996) 16410-16418.
- 6 [237] E. Caldin, *The Mechanisms of Fast Reactions in Solution*, IOS Press, Amsterdam, The
7 Netherlands, 2003.
- 8 [238] I. Chorkendorff, J.W. Niemantsverdriet, *Concepts of Modern Catalysis and Kinetics*, Wiley-VCH,
9 Weinheim, 2007.
- 10 [239] L.F. Phillips, Collision-theory calculations of rate constants for some atmospheric radical
11 reactions over the temperature range 10-600 K, *Journal of Physical Chemistry*, 94 (1990) 7482-7487.
- 12 [240] K.L.J. Lee, A mechanistic modeling of CO₂ corrosion of mild steel in the presence of H₂S, in:
13 *College of Engineering and Technology, Ohio University, Athens OH, 2004.*
- 14 [241] T.E. Graedel, Gildes model studies of aqueous chemistry. I. Formulation and potential
15 applications of the multi-regime model, *Corrosion Science*, 38 (1996) 2153-2180.
- 16 [242] S. Nestic, K.L.J. Lee, A mechanistic model for carbon dioxide corrosion of mild steel in the
17 presence of protective iron carbonate films - Part 3: Film growth model, *Corrosion: Journal of
18 Science and Engineering*, 59 (2003) 616-628.
- 19 [243] W. Sun, S. Nestic, A Mechanistic model of H₂S corrosion of mild steel, in: *Corrosion 2007
20 Conference & Expo, NACE International, Nashville TN, 2007, pp. Paper No. 07655.*
- 21 [244] J. Tidblad, T. Aastrup, C. Leygraf, GILDES model studies of aqueuos chemistry, *Journal of The
22 Electrochemical Society*, 152 (2005) B178-B185.
- 23 [245] N. Castin, M.I. Pascuet, L. Malebra, Modeling the first stages of Cu precipitation in a-Fe using a
24 hybrid atomistic kinetic Monte carlo approach, *The Journal of Chemical Physics*, 135 (2011) 064502.
- 25 [246] Y. Yang, S. Meng, L.F. Xu, E.G. Wang, S. Gao, Dissolution dynamics of NaCl nanocrystal in liquid
26 water, *Physical Review E*, 72 (2005) 012602.
- 27 [247] E. McCafferty, *Introduction to Corrosion Science*, Springer, New York, 2010.

- 1 [248] D. Chidambaram, M.J. Vasquez, G.P. Halada, C.R. Clayton, Studies on the repassivation
2 behavior of aluminum and aluminum alloy exposed to chromate solutions, *Surface and Interface*
3 *Analysis*, 35 (2003) 226-230.
- 4 [249] E.-A. Cho, C.-K. Kim, J.-S. Kim, H.-S. Kwon, Quantitative analysis of repassivation kinetics of
5 ferritic stainless steels based on the high field ion conduction model, *Electrochimica Acta*, 45 (2000)
6 1933-1942.
- 7 [250] J.C. Scully, in: Z.A. Foroulis (Ed.) *Environment sensitive fracture of engineering materials*, AIME,
8 New York, 1979.
- 9 [251] F.M. Song, K.S. Raja, D.A. Jones, A film repassivation kinetic model for potential-controlled
10 slower electrode straining, *Corrosion Science*, 48 (2006) 285-307.
- 11 [252] A. Anderko, N. Sridhar, D.S. Dunn, A general model for the repassivation potential as a function
12 of multiple aqueous solution species, *Corrosion Science*, 46 (2004) 1583-1612.
- 13 [253] A. Anderko, N. Sridhar, M.A. Jakab, G. Tormoen, A general model for the repassivation
14 potential as a function of multiple aqueous species. 2. Effect of oxyanions on localized corrosion of
15 Fe-Ni-Cr-Mo-W-N alloys, *Corrosion Science*, 50 (2008) 3629-3647.
- 16 [254] S.-J. Ahn, D.-Y. Kim, H.-S. Kwon, Analysis of repassivation kinetics of Ti based on the point
17 defect model, *Journal of the Electrochemical Society*, 153 (2006) B370-B374.
- 18 [255] P.-Q. Wu, J.-P. Celis, Ion Conduction Model Applied to Repassivation Kinetics of Tribo-Activated
19 Surfaces, *Journal of the Electrochemical Society*, 151 (2004) B551-B557.
- 20 [256] P.I. Marshall, G.T. Burstein, The effects of pH on the repassivation of 304L stainless steel,
21 *Corrosion Science*, 23 (1983) 1219-1228.
- 22 [257] C.-J. Park, H.-S. Kwon, Comparison of repassivation kinetics of stainless steels in chloride
23 solutions, *Metals and Materials International*, 11 (2005) 309-312.
- 24 [258] E. Schroder, R. Fasel, A. Kiejna, Mg(0001) surface oxidation: A two-dimensional oxide phase,
25 *Physical Review B*, 69 (2004) 193405.
- 26 [259] Y.A. Popov, Theory of pit nucleation. II- Interaction between pits at the early stage of
27 development. The role of solvent., *Protection of Metals*, 44 (2008) 126-133.
- 28 [260] T.T. Lunt, J.R. Scully, V. Brusamarello, A.S. Mikhailov, J.L. Hudson, Spatial interactions among
29 localized corrosion sites. Experiments and modeling, *Journal of The Electrochemical Society*, 149
30 (2002) B163-B173.

- 1 [261] S.P. White, D.P. Krouse, N.J. Laycock, Numerical simulation of pitting corrosion: intercatations
2 between pits in potentiostatic condtions, ECS Transactions, 16 (2006) 37-45.
- 3 [262] D.G. Harlow, R.P. Wei, A probability model for the growth of corrosion pits in aluminum alloys
4 induced by constituent particles, Engineering Fracture Mechanics, 59 (1998) 305-325.
- 5 [263] W.A. Curtin, R.E. Miller, Atomistic/continuum coupling in computational materials science,
6 Model Simul Mater Sc, 11 (2003) R33-R68.
- 7 [264] G. Makov, C. , C. Gattinoni, A. De Vita, Ab initio based multiscale modelling for materials
8 science, Model Simul Mater Sc, 17 (2009) 084008.
- 9 [265] G.C. Ganzenmüller, S. Hiermaier, M.O. Steinhauser, Energy-based coupling of smooth particle
10 hydrodynamics and molecular dynamics with thermal fluctuations, The European Physical Journal
11 Special Topics 206 (2012) 51-60.
- 12 [266] R.J. LeVeque, Finite Difference Methods for Ordinary and Partial Differential Equations - Steady
13 State and Time Dependent Problems, Society for Industrial and Applied Mathematics, Philadelphia,
14 2007.
- 15 [267] O.C. Zienkiewicz, R.L. Taylor, The finite element method, McGraw-Hill, London, 1977.
- 16 [268] S.V. Patankar, Numerical Heat Transfer and Fluid Flow, Hemisphere Publishing Company,
17 Washington DC, 1980.
- 18 [269] V.R. Voller, Basic control volume finite element methods for fluids and solids, World scientific,
19 Singapore, 2009.
- 20 [270] L. Bartosik, D. di Caprio, J. Stafiej, Cellular automata approach to corrosion and passivity
21 phenomena, Pure and Applied Chemistry 85 (2012) 247-256.
- 22 [271] M. Stratmann, H. Streckel, On the atmospheric corrosion of metals which are covered with thin
23 electrolyte layers-I. Verification of the experimental technique, Corrosion Science, 30 (1990) 681-
24 696.
- 25 [272] M.S. Venkatraman, I.S. Cole, B. Emmanuel, Corrosion under a porous layer: A porous electrode
26 model and its implications for self-repair, Electrochimica Acta 56 (2011) 8192-8203.
- 27 [273] A.M. Tartakovsky, et al. , Simulations of reactive transport and precipitation with smoothed
28 particle hydrodynamics, Journal of Computational Physics 222 (2007) 654-672.

- 1 [274] H.e.a. Grubmüller, Generalized Verlet algorithm for efficient molecular dynamics simulations
2 with long-range interactions, *Molecular Simulation* 6(1991) 121-142.
- 3 [275] W.G. Hoover, Isomorphism linking smooth particles and embedded atoms, *Physica A:
4 Statistical Mechanics and its Applications* 260 (1998) 244-254.
- 5 [276] C. Bataillon, F. et al. . Numerical methods for the simulation of a corrosion model with moving
6 oxide layer, *Journal of Computational Physics*, 231 (2012) 6213-6231.
- 7 [277] J.S. Newman, K.E. Thomas-Alyea, *Electrochemical systems*, John Wiley & Sons Inc., Hoboken,
8 NJ, 2004.
- 9 [278] I.S. Cole, e. al, *Holistic model for atmospheric corrosion Part 4 - Geographic information system
10 for predicting airborne salinity*, *Corrosion Science and Technology*, 39 (2004) 89-96.
- 11 [279] I.S. Cole, e. al., *Multiscale modelling of the corrosion of metals under atmospheric corrosion*,
12 *Electrochimica Acta*, 56 (2011) 1856-1865.
- 13 [280] I.S. Cole, D.A. Paterson, *Mathematical models of dependence of surface temperatures of
14 exposed metal plates on environmental parameters*, *Corrosion Engineering Science and Technology*,
15 41 (2006) 67-76.
- 16 [281] I.S. Cole, D.A. Paterson, W.D. Ganther, *Holistic model for atmospheric corrosion Part 1 –
17 Theoretical framework for production, transportation and deposition of marine salts*, *Corrosion
18 Engineering, Science and Technology*, 38 (2003) 129-134.

19

20